

# Radiation Hardness Assurance for Space Systems

**Christian Poivey**  
**SGT-Inc.**  
**NASA GSFC**

1.0	Introduction .....	2
2.0	Radiation Hardness Assurance Overview.....	2
3.0	Define the Space Radiation Environment.....	4
3.1	External Environment.....	4
3.1.1	Introduction.....	4
3.1.2	Environments.....	4
3.1.3	Trapped radiation belts models.....	5
3.1.4	Solar Particle Event models.....	7
3.1.5	Galactic Cosmic Rays environment models.....	9
3.1.6	Spacecraft secondary radiation.....	9
3.2	Environment within the Spacecraft.....	10
3.2.1	Introduction.....	10
3.2.2	Total Ionizing Dose (TID).....	11
3.2.3	Single Event Effects.....	17
3.2.4	Displacement Damage.....	19
4.0	Bound the Part Response.....	20
4.1	Introduction.....	20
4.2	Use of existing Radiation Data.....	22
4.3	Testing.....	22
4.3.1	Total Dose Testing.....	22
4.3.2	Single Event Effect testing.....	27
4.3.3	Bulk damage, displacement effect testing.....	31
5.0	Define the system/subsystem response to the radiation environment- Parts categorization.....	32
5.1	General.....	32
5.2	Total ionizing dose.....	32
5.2.1	Define the radiation failure level.....	32
5.2.2	Define the radiation specification/levels.....	33
5.2.3	Parts categorization.....	36
5.3	Displacement Damage.....	38
5.4	Single Event Effects.....	39
5.4.1	General.....	39
5.4.2	Error rate Prediction.....	39
5.4.3	Criticality analysis.....	40
5.4.4	Particular case: Error rate prediction not possible.....	48
6.0	Management of Hardness Assurance.....	48
6.1	Introduction.....	48
6.2	Radiation specifications.....	49
6.2.1	Introduction.....	49
6.2.2	Radiation Environment specification.....	49
6.2.3	Radiation Hardness assurance specification.....	50
6.3	Radiations reviews.....	50
6.4	Waivers.....	51
7.0	Emerging Radiation Hardness Assurance Issues.....	51
8.0	Conclusion.....	52
9.0	Acknowledgements.....	52
10.0	References.....	53

## 1.0 INTRODUCTION

The space radiation environment can lead to extremely harsh operating conditions for on-board electronic box and systems. The characteristics of the radiation environment are highly dependent on the type of mission (date, duration and orbit). Radiation accelerates the aging of the electronic parts and material and can lead to a degradation of electrical performance; it can also create transient phenomena on parts. Such damage at the part level can induce damage or functional failure at electronic box, subsystem, and system levels. A rigorous methodology is needed to ensure that the radiation environment does not compromise the functionality and performance of the electronics during the system life. This methodology is called hardness assurance. It consists of those activities undertaken to ensure that the electronic piece parts placed in the space system perform to their design specifications after exposure to the space environment. It deals with system requirements, environmental definitions, part selection, part testing, shielding and radiation tolerant design. All these elements should play together in order to produce a system tolerant to the radiation environment.

An overview of the different steps of a space system hardness assurance program is given in section 2. In order to define the mission radiation specifications and compare these requirements to radiation test data, a detailed knowledge of the space environment and the corresponding electronic device failure mechanisms is required. The presentation by J. Mazur deals with the Earth space radiation environment as well as the internal environment of a spacecraft. The presentation by J. Schwank deals with ionization effects, and the presentation by T. Weatherford deals with Single particle Event Phenomena (SEP) in semiconductor devices and microcircuits. These three presentations provide more detailed background to complement the sections 3 and 4. Part selection and categorization are discussed in section 5. Section 6 presents the organization of the hardness assurance within a project. Section 7 discusses emerging radiation hardness assurance issues.

## 2.0 RADIATION HARDNESS ASSURANCE OVERVIEW

Figure 1 gives an overview of the radiation hardness assurance process. A short description of the different steps follows with details given in the subsequent chapters. This process is iterative. It starts first with top-level estimations of the radiation environment, then the radiation levels are refined and the electronic designs analyzed in order to validate the most sensitive parts.

- A. Description of the mission radiation environment and definition of the radiation levels within the spacecraft: The particle spectra (heavy ion Linear Energy Transfer (LET) spectra, proton and electron spectra and dose-depth curves) for the specific mission are defined. This will be used for the definition of the radiation levels within spacecraft and/or the radiation specification levels.
- B. Assessment on parts radiation sensitivity: The radiation hardness of the parts is estimated on the basis of radiation databases and relevant radiation tests.
- C. Radiation aspects in Worst Case Analysis (WCA) of system and circuit design: Parts radiation sensitivity data is used to perform a worst-case analysis of the circuit design. The overall equipment and spacecraft worst case performance over the mission length, taking into account radiation effects, aging and other causes of

degradation is estimated. By combining the system application of each part and its radiation response, a radiation failure level can be determined for each part.

D. Part categorization: The radiation failure of each part is compared to its mission radiation level or the radiation requirements and a decision is made concerning the hardness of those devices in the system. The part categorization is the key activity of a hardness assurance program. The factor used to select which category the part falls into for each radiation environment is the Radiation Design Margin (RDM). RDM is defined as the ratio of the part failure level to the part radiation environment. When the part hardness greatly exceeds the system requirements, the part is not hardness critical and can be used in this application without any further action.

- When the part hardness is lower than the radiation level ( $RDM < 1$ ), the part can not be used as is and risk reduction tasks should be performed.
  - **Investigation:** A more accurate estimation of the radiation level (e.g. using a 3 D Monte-Carlo code to calculate the total dose level received by the part) may allow a reduction of the radiation requirement. On the other hand, a complementary radiation test closer to the application conditions may also increase the radiation failure level of the part.
  - **System or equipment level countermeasure:** Countermeasures can be implemented to either increase the acceptable sensitivity level of the part or reduce the radiation environment: additional shielding at component level (spot shielding) or at box level (additional thickness of box cover), switching of redundant component or function, error correction system, specific memory organization, latch-up protection circuitry, etc.
  - **Part replacement:** The part is replaced by another part having a higher radiation tolerance.
- When the part hardness is not significantly higher than the system requirements, the part is considered radiation hardness critical. In order to minimize the risk associated with the spread of device hardness between manufacturing lots (and also within the same manufacturing lot), flight lot parts can be tested during procurement.

During the lifetime of a mission's design and development, multiple variables change. These include:

- updates to parts list
- revised spacecraft layout
- revised mission requirements such as mission duration
- addition of new payloads, or
- the discovery of new radiation effects information.

Due to these and other factors, many of the steps in the approach may be revisited throughout the mission's radiation hardness assurance program.

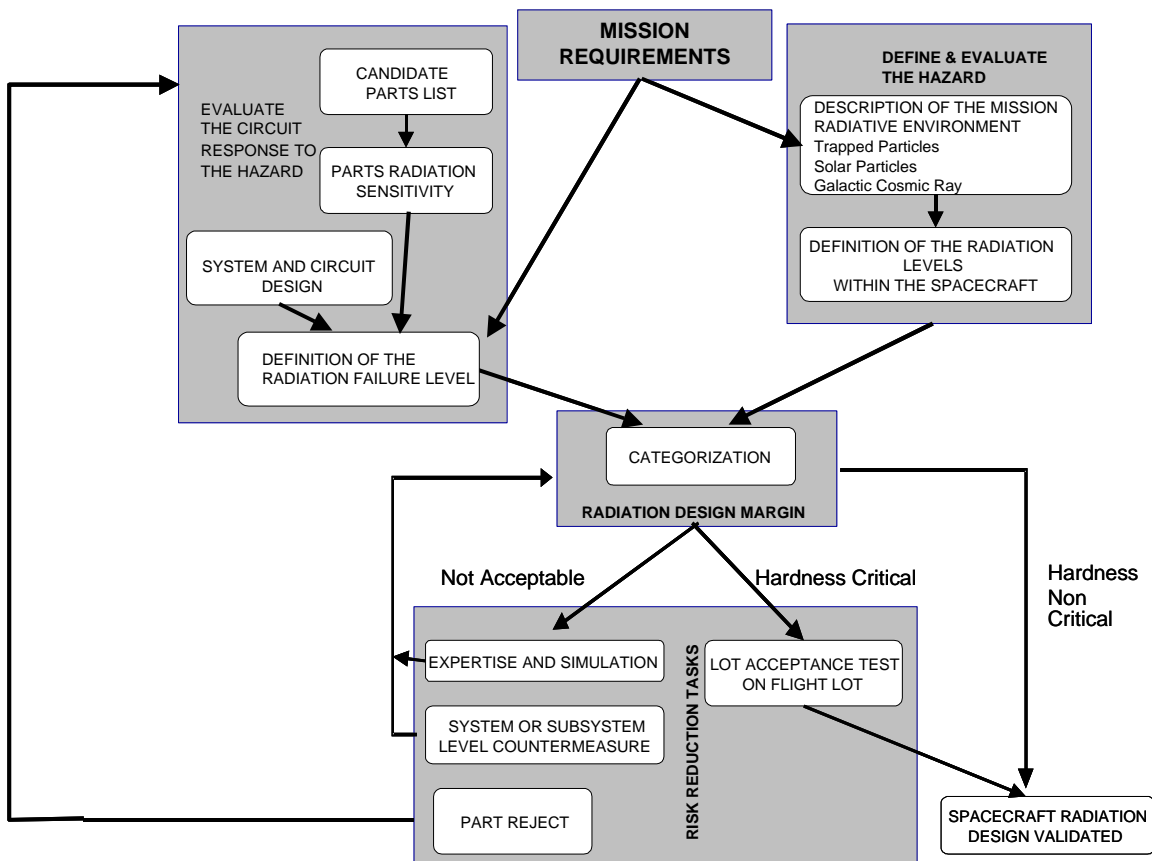


Figure 1: Overview of the radiation hardness assurance process.

### 3.0 DEFINE THE SPACE RADIATION ENVIRONMENT

#### 3.1 External Environment

##### 3.1.1 Introduction

It is important to define the radiation environment of a mission early in the design cycle. During the mission definition phase it is an element of trade-offs for orbit selection. When the mission is defined, the knowledge of the radiation environment will allow the estimation of the effort that shall be put into hardness assurance. The important mission definition information that is necessary to define accurately the radiation environment is:

- Orbital parameters of the mission allowing unambiguous definition of spacecraft orbit.
- Worst case number of transfer orbits, with their individual orbital parameters.
- Foreseen epoch for launch.
- Mission duration.

##### 3.1.2 Environments

The Earth space radiation environment is presented in detail in the first section of this short course. The reader interested in more details about the space radiation environment

should look at that and also at [Bart 97]. The three main sources of radiation that have to be considered are:

- The trapped electrons and protons in the radiation belts.
- The protons and heavy ions produced by the Solar Particle Events (SPE).
- The Galactic Cosmic Rays protons and heavy ions.

The plasma sphere environment is generally not a hazard to most spacecraft electronics. However it is damaging to surface materials and differentials in the plasma environment can contribute to spacecraft surface charging and discharging problems [Holm 93].

Other radiation sources need to be considered for some specific missions or systems (for example, the neutrons resulting from the energetic particle interactions with the atmosphere in the case of low-altitude missions).

### **3.1.3 Trapped radiation belts models**

The standard models of radiation belt energetic particles are the AE-8 and AP-8 models for electrons [Vett 91] and protons [Saw 76], respectively. The AP-8 model for protons gives proton fluxes from 0.1 to 400 MeV while the AE-8 model for electrons covers electrons from 0.04 to 7 MeV. These models give omni-directional fluxes as functions of idealized geomagnetic dipole coordinates  $B/B_0$  and  $L$  ( $B$  is the magnetic field strength and  $L$  is the value that marks the particle drift shells by their magnetic equatorial distance from the center of the Earth). They are used with an orbit generator and a geomagnetic field computation to give instantaneous or orbit-averaged fluxes. The user defines an orbit, generates a trajectory, transforms it to geomagnetic coordinates, and accesses the radiation belt models to compute the flux spectra. Apart from separate versions for solar maximum and solar minimum, there is no description of the temporal behavior of fluxes. The trapped particle models represent omnidirectional, integral intensities that one would expect to accumulate on average over a six months period of time [Bart 97]. For limited durations, short-term excursions from the model's averages can reach orders of magnitude above or below. For example, at high altitudes in particular (e.g. around geostationary orbit) fluxes vary by orders of magnitude over short times and exhibit significant diurnal variations; the models do not describe these. In addition, the models do not contain any explicit flux directionality.

At low altitudes, on the inner edge of the radiation belts, particle fluxes rise very steeply with altitude and small errors in computing locations can give rise to large errors in particle fluxes. This is a problem since the geomagnetic field is shifting and decaying so that the situation is no longer the same as when the model data were acquired. Use of a geomagnetic field model other than the one used in generating the model can result in large flux errors at low altitude. Therefore, the models should only be used together with the geomagnetic field models shown in Table 1 [Bart 97].

Although the use of an old field model and epoch can reduce errors in the magnitudes of fluxes, it should be noted that this does not model the spatial locations of radiation-belt features (e.g. the position of the South Atlantic Anomaly (SAA)), or particle fluxes, as they are today. This error is usually averaged out when the fluence is orbit integrated over

a period of 24 hours or greater but it can result in errors when specific positions in space are analyzed.

Table 1: Standard field models to be used with radiation belt models

Radiation-belt model	Geomagnetic field model
AE-8-MIN	Jensen-Cain 1960
AE-8-MAX	Jensen-Cain 1960
AP-8-MIN	Jensen-Cain 1960
AP-8-MAX	GSFC 12/66 extrapolated to 1970

Figures 2 and 3 show examples of trapped electrons and protons spectra, respectively. These examples are for a 590 km altitude and 29 degrees inclination orbit with a mission duration of 5 years.

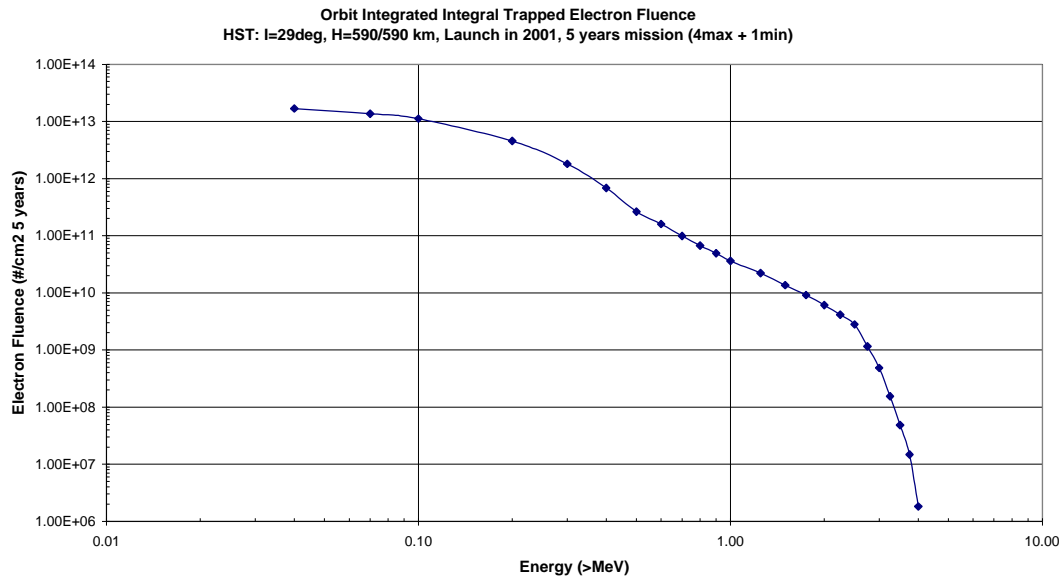


Figure 2: Example of a trapped electron spectrum.

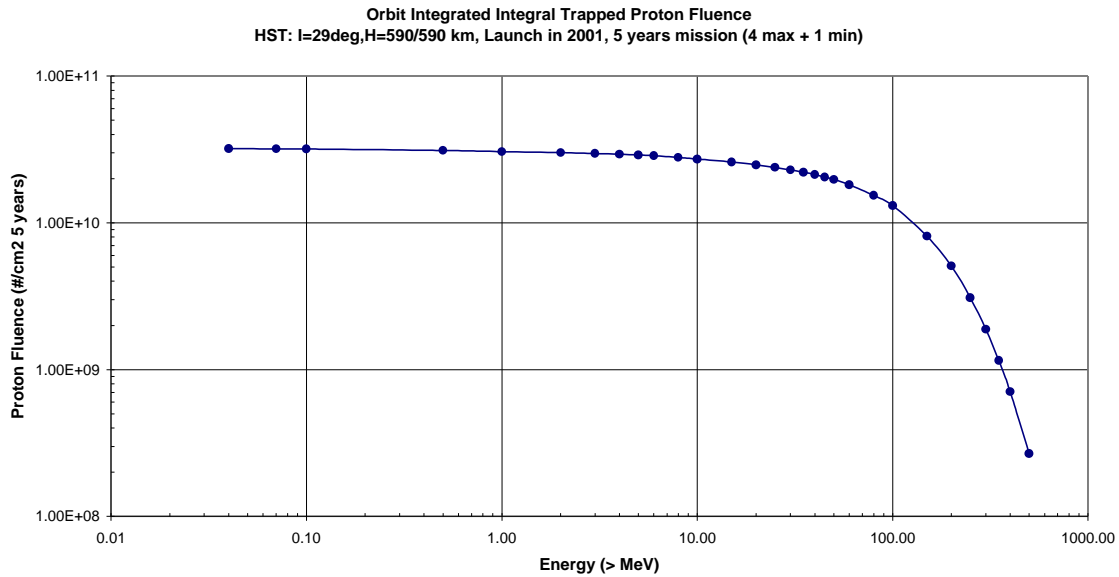


Figure 3: Example of a trapped proton spectrum.

At low altitude ( $< 1000$  km), actual measurements of the trapped protons fluxes are 60 to 500% higher than those predicted by the AP8 models. Daly [Daly 96] determined that a large part of this error is due to the method used to interpolate between the  $B/B_0$  values in the regions near the atmospheric cut-off. Huston [Hust 98] analyzed environment data for the TIROS/NOAA satellite in order to produce a low altitude proton model based on coordinates more applicable to this region in space and also a more accurate representation of the effect of solar cycle modulation. Figure 4 compares the AP8 models and the Huston model orbit averaged proton fluxes measurements from 1986 to 1996 for the Hubble Space Telescope (HST) orbit (690 km circular orbit, 29 degrees inclination). We can see that the AP8 model underestimates the proton flux by at least a factor of 3 for this orbit. One may want to use this model in order to apply correction factors on the AP8-model.

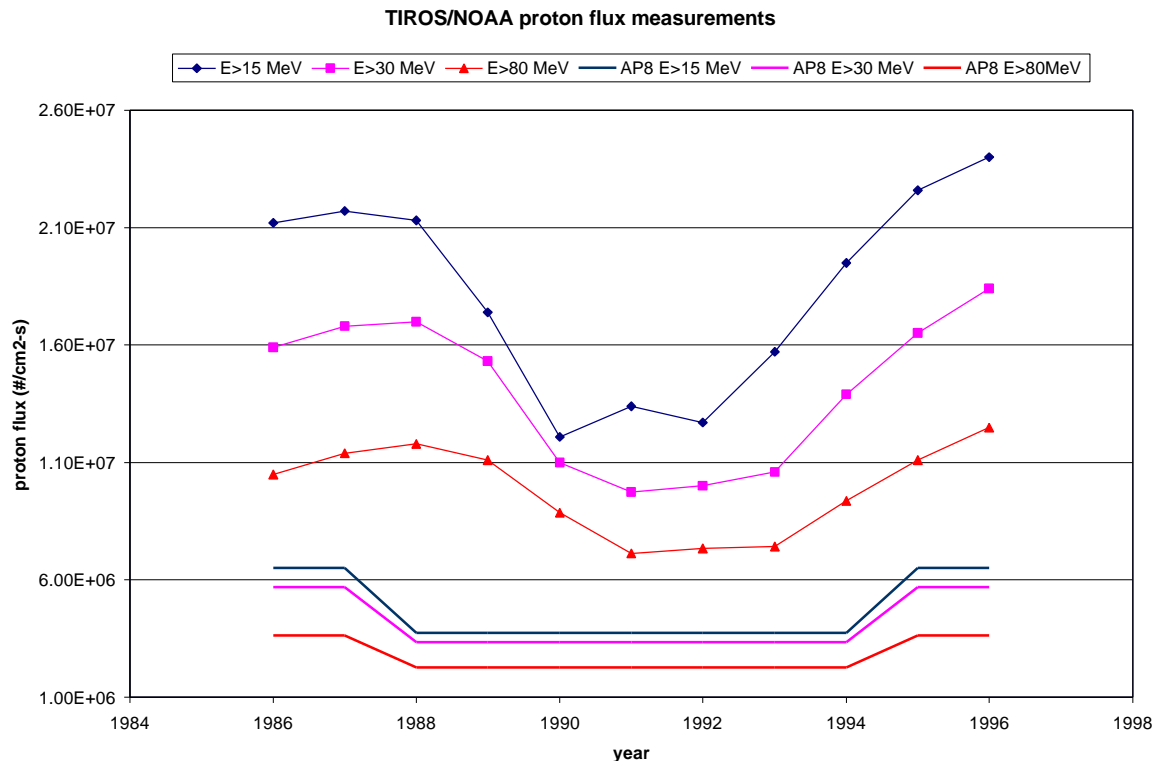


Figure 4: Comparison of the Huston model with the AP8 model, for the HST orbit.

### 3.1.4 Solar Particle Event models

#### 3.1.4.1 Standard models for mission integrated proton fluences

During energetic events on the Sun, large fluxes of energetic protons are produced which can reach the Earth. Solar particle events, because of their unpredictability and large variability in magnitude, duration and spectral characteristics, have to be treated statistically. Two models are available:

- The JPL-1991 model [Feyn 93].
- The Emission of Solar Proton (ESP) model [Xaps 00].

The JPL-1991 model is based on data from solar cycles 20, 21 and part of 22. The ESP model incorporates the whole 3 cycles, which tends to make predicted proton fluences slightly higher, as shown in Figure 5. The JPL-1991 model provides data up to 60 MeV. The ESP model extends this energy range up to 300 MeV and therefore covers all the energy range of interest.

These models are the standard models used for engineering consideration of time-integrated effects. Since these are statistical models, a probability level needs to be entered. Table 2 gives the recommended confidence levels in function of the mission exposure to solar maximum conditions. They are based on an analysis of worst-case periods [Tran 92].

Table 2: Recommended confidence levels as a function of the number of years of mission exposure to Solar maximum conditions [Tran 92].

Number of years of exposure	Probability level (%)
1	97
2	95
3	95
4	90
5	90
6	90
7	90

Figure 5 compares the 2 models for the 90% confidence levels. The ESP model is the standard model used at NASA-GSFC.

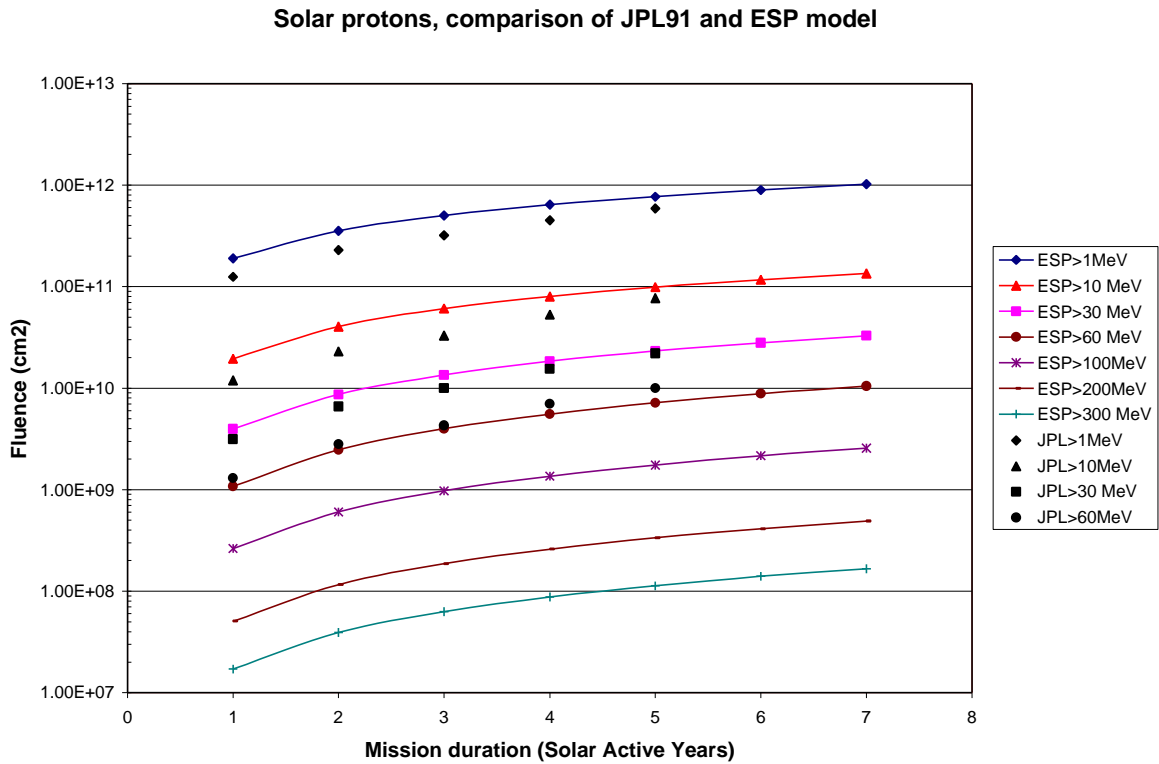


Figure 5: Comparison of the ESP and JPL-91 models for a 90% confidence level [Xaps 00].

### **3.1.4.2 Spectrum of individual proton events**

The August 1972 event produced a peak flux near the Earth in excess of  $10^6$  protons  $\text{cm}^{-2} \text{s}^{-1}$  above 10 MeV energy, while the October 1989 event produced a peak flux of about  $10^5$  protons  $\text{cm}^{-2} \text{s}^{-1}$ . The fluence spectra of these 2 events are generally used to represent a worst-case proton event classified as extremely large [Stas 96]. For Single Event Upset analysis, the October 1989 model integrated in CREME 1996 is the standard model.

Burrell developed a modified Poisson statistics to describe the probability  $p$  of a number of events  $n$  occurring during a time  $t$  [Kin 74]. This is sometimes useful in considering numbers of events in contrast to the total fluence. Generally during 7 years of Solar maximum activity, no more than 5 extremely large events could occur with a 90% confidence level.

A probability model for worst-case solar proton event fluence has also been integrated in the Emission of Solar Proton model (ESP) [Xaps 99-1].

### **3.1.4.3 Solar particle event ions**

The CREME96 model is the standard model for Solar Particle Event ions. CREME96 contains models based on the October 1989 event. It provides models of energy spectrum, composition and LET spectrum for the worst week, worst day and peak 5 minutes [Tylk 97].

### **3.1.5 Galactic Cosmic Rays environment models**

Cosmic Ray environment models were originally created by Adams and co-workers at the US Naval Research Laboratory [Adam 86], under the name CREME. They provided a comprehensive set of Cosmic Ray and Solar event ion LET and energy spectra including treatment of geomagnetic shielding and material shielding. CREME has been superseded by CREME96 [Tylk 97]. The major differences are in the inclusion of a model of the Cosmic Ray environment and its solar-cycle modulation, improved geomagnetic shielding calculation, improved material shielding calculation and more realistic Solar Energetic Particle Event ion environments. Cosmic ray fluxes are anti-correlated with solar activity so the highest cosmic ray fluxes occur at solar minimum. CREME 96 is the standard model for cosmic ray environment assessment. Ions from  $Z=1$  to 92 should be included to define the mission GCR environment.

### **3.1.6 Spacecraft secondary radiation**

Secondary radiation is created by the transport of primary particles through the spacecraft materials. For engineering purposes it is often only electron-induced bremsstrahlung radiation that is considered as a significant secondary radiation source. In special cases other secondaries need to be considered.

In evaluating the radiation background effects in detector systems, it is often secondary radiation that is important [ECSS 00]. Most radiation is emitted at the instant of interaction (“prompt”) while some is emitted some time after a nucleus has been excited by an incoming particle (induced radioactivity).

By its nature, secondary radiation is analyzed on a case-by-case basis, possibly through Monte-Carlo simulations. For engineering estimates of bremsstrahlung, the SHIELDOSE [Selt 80] model can also be used.

## 3.2 Environment within the Spacecraft

### 3.2.1 Introduction

In engineering a space system to operate in the space environment, it is necessary to relate the environment to system degradation quantitatively. The Table 3 gives the parameters that should be determined for quantification of the various radiation effects. Although some of these parameters are readily derivable from a specification of the environment, others either need explicit consideration of test data or the detailed consideration of interaction geometry and mechanisms.

It is very important to define accurately the radiation levels within a spacecraft. Over specification leads to unnecessary costs and delays, under specification may involve very expensive retrofits or compromise the mission.

Table 3: Parameters for quantification of radiation effects.

<b>Radiation effect</b>	<b>Parameter</b>
CMOS Electronic component degradation	Total ionizing dose (TID)
Bipolar Electronic component degradation	TID and Displacement Damage Dose (DDD) or equivalent fluence for a selected proton energy
Material degradation	TID and DDD or equivalent fluence for a selected proton energy (bulk damage)
Opto-electronic component degradation	TID and DDD or equivalent fluence for a selected proton energy
Solar cell degradation	Displacement damage equivalent fluence for a selected electron/proton energy or DDD
Single Event Effect (SEE)	Ions LET spectra, proton energy spectra
Sensor interference (background signals)	Flux above energy threshold or flux threshold
Internal electrostatic charging	Electron flux and fluence

## **3.2.2 Total Ionizing Dose (TID)**

### **3.2.2.1 Introduction**

Total dose levels to be received at component die level are calculated for active parts, taking into account spacecraft shielding. Figure 6 shows an overview of a radiation transport analysis. Total dose simulations can be performed either using 3 D sector based codes or 3D Monte Carlo transport codes. Sector based codes are simple to use and provide results with low computation time while Monte Carlo codes are time consuming but much more accurate. Monte Carlo techniques numerically plot the trajectories of large numbers of particles and predict their interactions in the material through which they are traveling. Interactions usually have a distribution of possible outcomes to which random sampling is applied. For electrons, successive interactions are too numerous to follow individually; instead, attention is given to a small section of the electron's path containing a large number of individual interactions. The net result of all the interactions can be expressed analytically and at the end of each section, the electron energy loss is computed and its direction is altered by random sampling of a scattering distribution. The section length is chosen such that the energy loss in the section is a small fraction of the electron energy.

Monte Carlo techniques can also be used to compute the transport and interaction of other particles and their secondaries, including bremsstrahlung and neutrons.

Even when a Monte-Carlo analysis is performed, a dose-depth curve is calculated to define the top-level requirements at the beginning of the program.

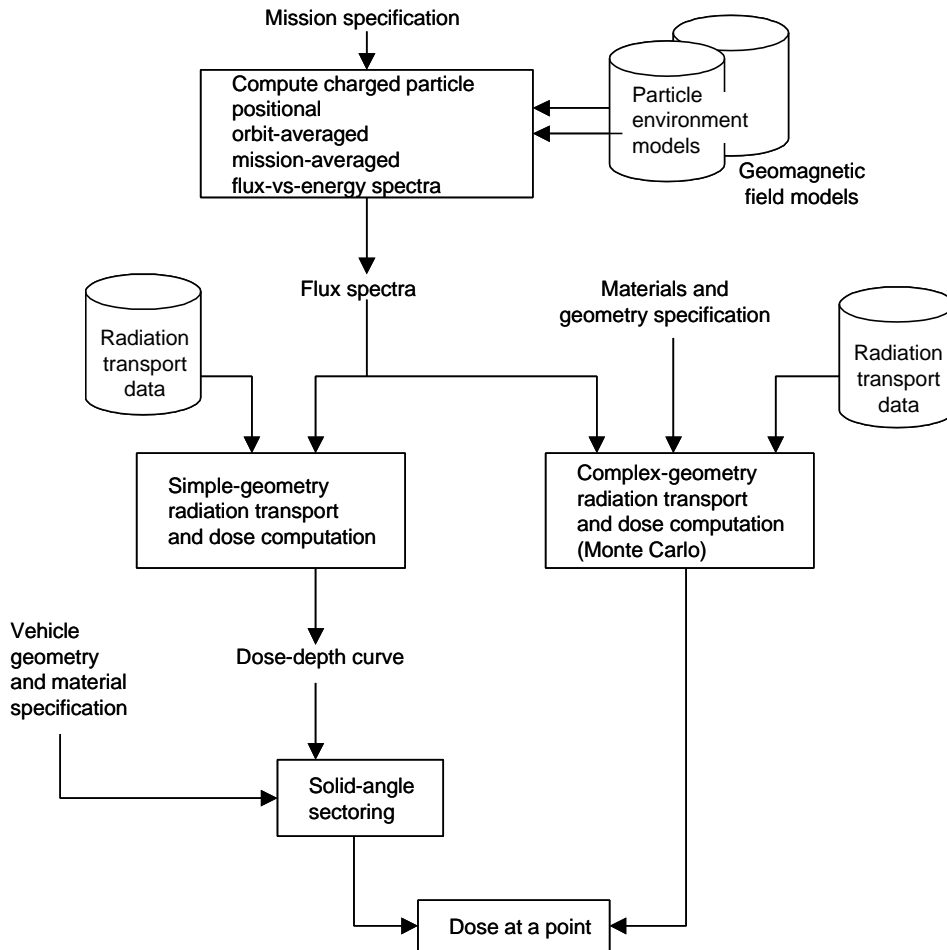


Figure 6: Radiation transport analysis overview, from [Daly 1989].

### 3.2.2.2 Top level estimation, dose depth curve

The top-level ionizing dose environment is represented by the dose depth curve. This can provide dose as a function of shield thickness in a planar geometry or as a function of spherical shielding about a point. The spherical model gives a conservative estimate of the dose received. The planar model is appropriate for surface materials or for locations near to a planar surface [ECSS 2000]. In general electronic components are not in such a location and a spherical model is recommended for general specification. Figure 7 illustrates two typical 1D sphere geometries: the solid sphere model and the shell sphere model.

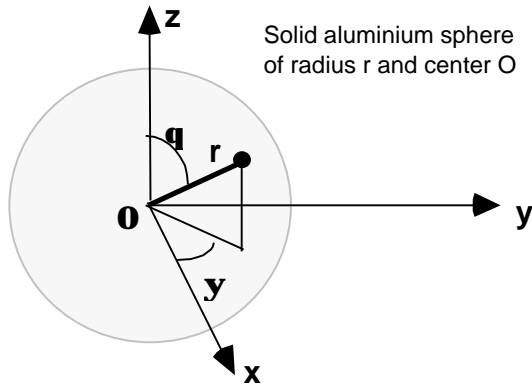


Figure 7-a : Solid sphere 1-D shielding model. The dose depth curve  $D(r)$  based on solid sphere gives the total dose to be received at center O of an Al solid sphere (O,r), when inside a given radiation environment.

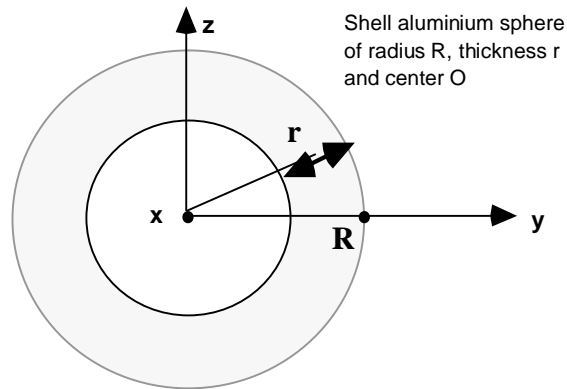


Figure 7-b : Shell sphere 1-D shielding model (Y,Z plan). The dose depth curve  $D(r)$  based on shell sphere gives the total dose to be received at center O of the aluminum shell having center O, radius R and thickness r, when inside a given radiation environment.

The dose depth curve could be calculated either with a Monte Carlo code or with the SHIELDOSE model. The SHIELDOSE model is based on a large data set containing the dose per unit of incident fluence as a function of depth of Aluminum shielding and particle energy [Seltz 80]. Datasets have been collected with Monte Carlo codes on simple geometries (e.g. slab, solid spheres). NOVICE [Jord 1982] is an example of a Monte Carlo code widely used in the industry for radiation analysis. GEANT4 is also a Monte Carlo code that is used [Trus2000]. SHIELDOSE2 is integrated in the SPACERAD and SPENVIS radiation analysis computer tools.

The dose depth curve allows the definition of a top-level dose requirement for a specific mission assuming a conservative shielding thickness, for example 100 mils of Aluminum. This could be adequate for a low dose environment mission but generally the dose levels obtained are too high and a more accurate analysis is needed. Figure 8 shows the dose depth curve of the ST5 mission (elliptical orbit 200-35790 km altitude, 0 degree inclination and three months duration). The Figure shows the contribution of the different environments (trapped electrons and protons, solar protons and the bremsstrahlung) to the total dose. We can see in the figure that for this mission the electrons dominate the TID environment up to 250 mils of shielding and that they are nearly completely eliminated after 350 mils of shielding.

**Total dose at the center of Solid Aluminum Sphere**  
**ST5: 200-35790 km, 0 degree inclination, three months**

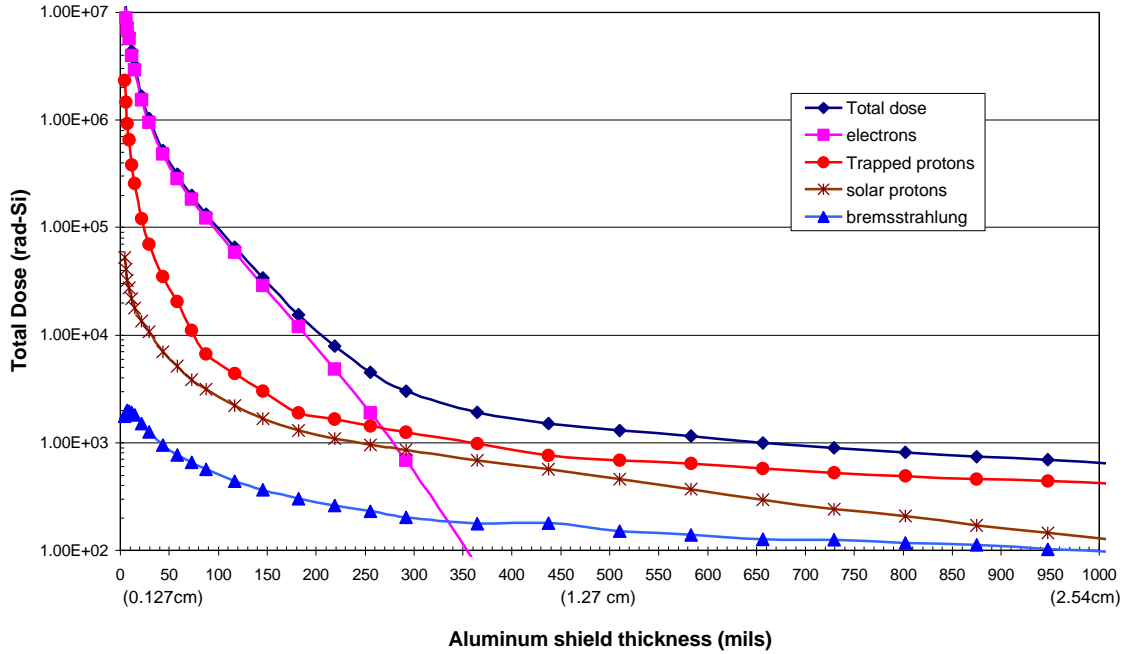


Figure 8: Example of a dose depth curve.

### 3.2.2.3 Sector Based analysis

The sectoring method traces rays through the shielding in a large number of directions. A sector based analysis needs two inputs, the 1 dimension dose depth curve and the 3 dimension structural model of the materials surrounding the sensitive component. The output of the sector based analysis is the total dose received at the sensitive component die level.

The ray trace methodology consists in calculating the dose at the center (called the detector in the following) of a parallelepiped. Ray tracing calculations follow the procedure described below:

- Each face is meshed  $N1 \times N2$  ( $9 \text{ min} \leq N_i \leq 20$ ),
- $M$  rays are launched from the detector, in the direction of a point of the meshing. The number of rays shall be at least 15 per mesh. For each ray  $k$ ,  $1 \leq k \leq M$ , the thickness of every surface encountered by the ray  $k$  is added and an equivalent Aluminum thickness  $t_{ijk}$  is then calculated. For each mesh element  $(i,j)$ , ( $1 \leq i \leq N1$ ,  $1 \leq j \leq N2$ ) a mean value  $t_{ij}$  is determined:

$$t_{ij} = \frac{1}{M} \sum_{k=1}^{k=M} t_{ijk}$$

From this value, the mean dose  $d_{ij}$  received per target through the mesh element  $(i,j)$  is deduced from the dose depth curve (which gives value over  $4\pi$  steradians):

$$d_{ij} = \frac{\Omega_{ij}}{4\pi} D(t_{ij})$$

$\Omega_{ij}$  is the solid angle with the mesh (i,j) as the base and the detector as the top. The dose  $d$  received on a face is the sum of the dose received on each mesh of the face:

$$d = \sum_{i=1}^{N1} \sum_{j=1}^{N2} d_{ij}$$

From this dose is deduced an equivalent thickness "  $t$  " from 1D dose depth curve  $D(t)$ :

$$D(t) = \frac{4pd}{\Omega}$$

$$\text{with } \Omega = \sum_{i=1}^{N1} \sum_{j=1}^{N2} \Omega_{ij}$$

2 techniques are possible to determine the thickness  $t$  crossed by a ray for an elemental sector: the NORM technique and the SLANT technique as described in Figure 9.

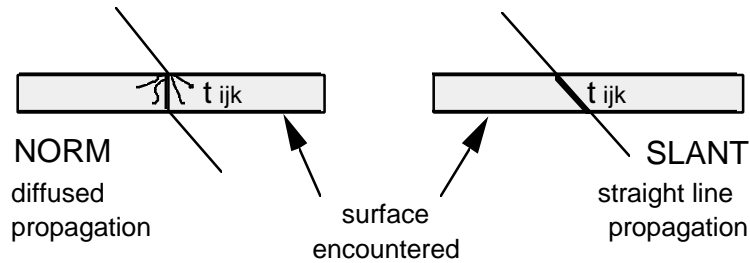


Figure 9: NORM and SLANT techniques for sector based analysis.

These two techniques lead to significantly different estimates of shielding thickness. As demonstrated by MonteCarlo validations and an analysis on ionizing particle transport, there is a limited range of application for each of these techniques [Astr 01]. Protons propagate in straight line, and proton shielding calculation can be performed using the SLANT method, while electrons propagate in an erratic way and electron shielding calculation need to be performed using the NORM technique.

When a 1D dose-depth curve is calculated with the shell sphere model, the sector analysis should use the NORM technique. When the solid sphere model is used, the sector analysis should use the SLANT technique. If this is not done, underestimations of the dose levels could result.

Figures 10 and 11 compare the results obtained with the 2 techniques for a geostationary and a low polar orbit environment respectively with a Monte Carlo analysis that gives the most accurate estimation. The dose levels have been calculated on a target within a package, within an electronic box in a spacecraft. The spacecraft and the box structures have been modeled. The same model has been used for the three different analyses. The shielding provided by the spacecraft and the electronic box is in the range of 2 to 4 g/cm<sup>2</sup>, which is representative of the shielding provided to most of the electronic parts used in a spacecraft. Four kinds of electronic parts packages have been analyzed: a metal TO39 package, a ceramic CQFP package, a plastic TSOP package, and a Radiation hardened package made of different layers of heavy and light materials.

The results show that the different analyses give significantly different results on an electron-dominated orbit like the geostationary case. The sector analysis could significantly overestimate or underestimate the dose levels.

For proton-dominated orbits like the LEO case, the effect of the analysis method is less significant. An accurate sector analysis will give a result within +/- 10% to the actual dose level.

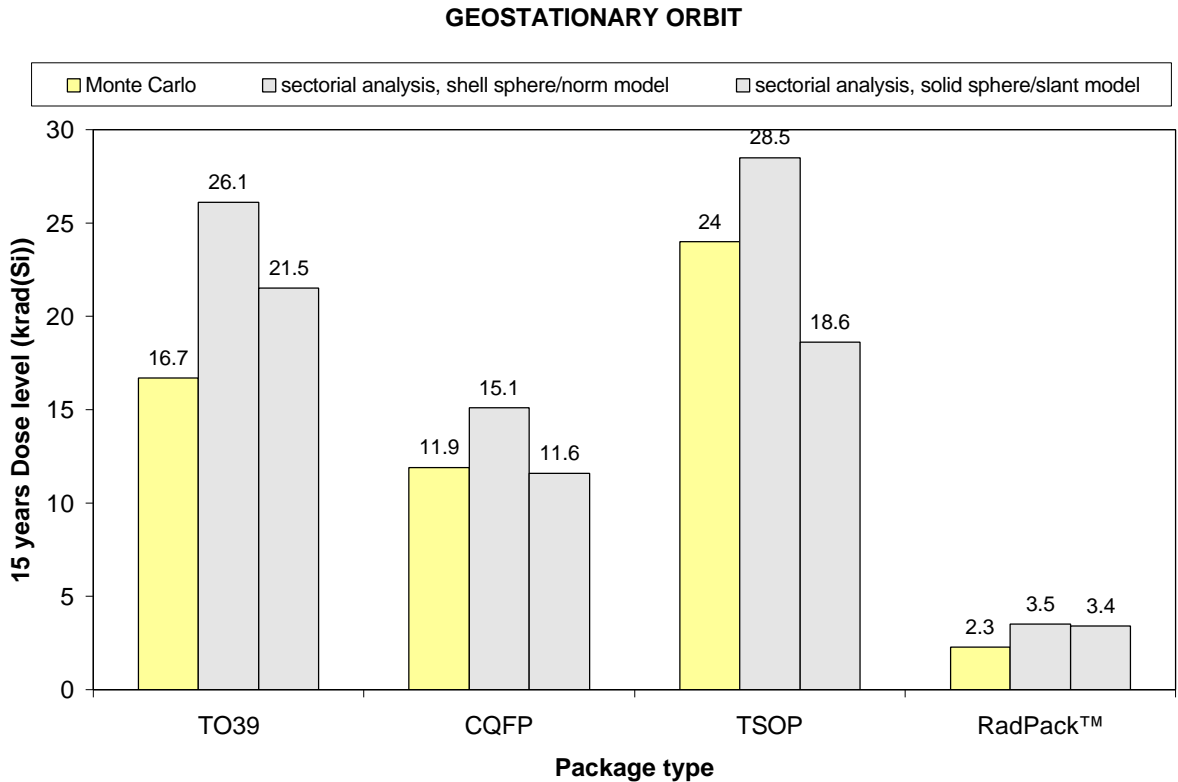


Figure 10: comparison of the results obtained with three different methods for a geostationary orbit [Astr 01].

### 3.2.2.4 3D Monte Carlo analysis

The 3D Monte Carlo analysis method gives the best estimate of the deposited dose. This is the method used and recommended by NASA-GSFC. However, the accuracy of the calculation depends on the number of particles that hit the target in the simulation. An acceptable level of accuracy is reached when a minimum of 1024 particles hit the target. Such a calculation may take a considerable amount of time (in the order of days), because a significant amount of particle needs to be analyzed in order to get 1024 that reach the target. A reverse Monte-Carlo code, like NOVICE, starts the analysis from the target and goes back to the external environment; so only 1024 particles need to be analyzed. This type of code will give accurate results significantly faster.

### LEO ORBIT (820 km/90 degrees)

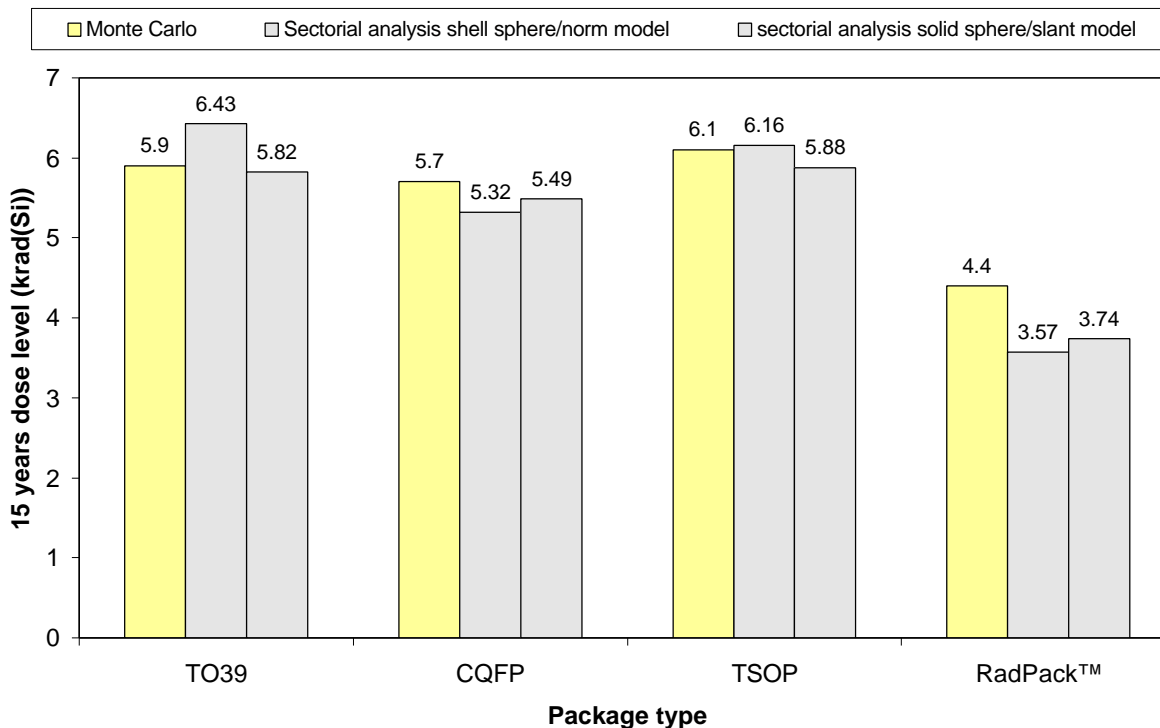


Figure 11: comparison of the results obtained with three different methods for a LEO polar orbit [Astr 2001].

### 3.2.3 Single Event Effects

Once the GCR spectra have been transported through a given value of shielding, changes of the shielding thickness do not have a significant effect on the GCR fluxes. But it could have an effect on solar event particles fluxes. Shielding also has a limited effect on protons of energy greater than 30 MeV. For single event studies the heavy ion LET spectra and proton energy spectra are calculated for a conservative value of shielding. At NASA-GSFC the spectra are calculated for an Aluminum shielding of 100 mils (2.54 mm). The European Space Agency recommends assuming a  $1\text{g/cm}^2$  of Aluminum (3.7 mm) [ECSS 00]. Figure 12 shows an example of GCR and SPE LET spectra for an interplanetary orbit. We can see that the heavy ion fluxes during SPE are significantly higher than the GCR background fluxes.

A spacecraft goes through the trapped proton belts during only a portion of the whole orbit. Therefore, an orbit averaged trapped proton flux does not describe correctly the trapped proton environment. For SEE analysis, the peak fluxes that correspond to the worst-case pass through the Van Allen belts need also to be calculated. Figure 13 shows an example of average and peak trapped proton energy spectra, indicating that these can differ by orders of magnitude.

**Integral LET Spectra at 1 AU (Z=1-92) for Interplanetary orbit  
100 mils Aluminum Shielding, CREME96**

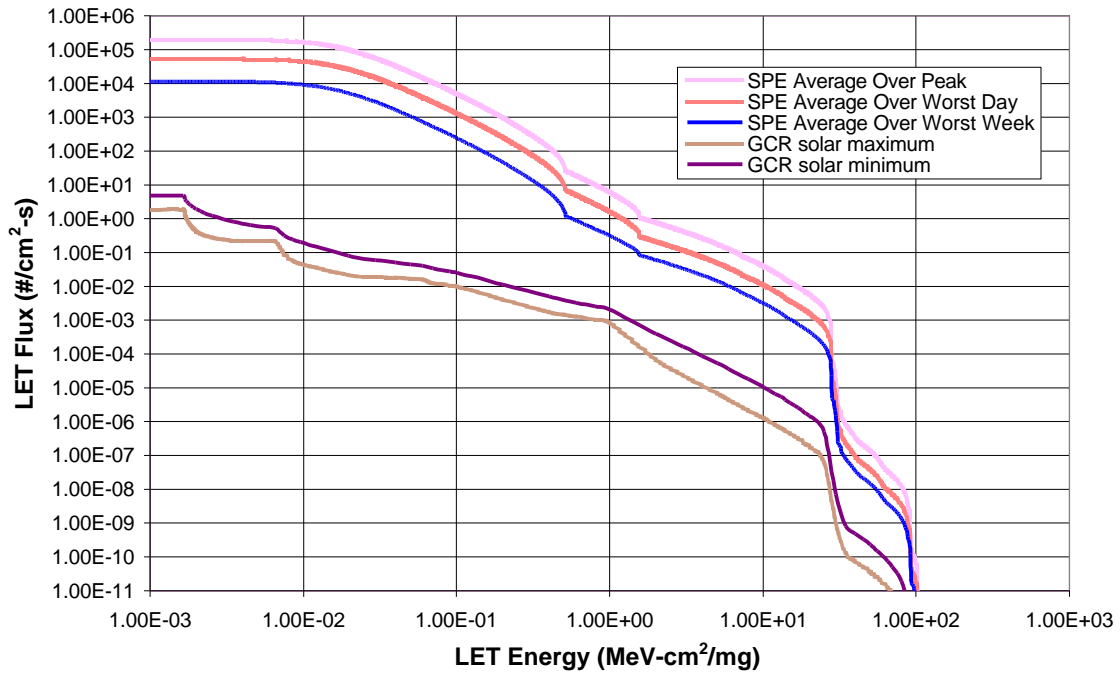


Figure 12: Example of GCR and SPE LET spectra.

**Trapped Proton Integral Fluxes, behind 100 mils of Aluminum shielding  
ST5: 200-35790 km 0 degree inclination , Solar maximum**

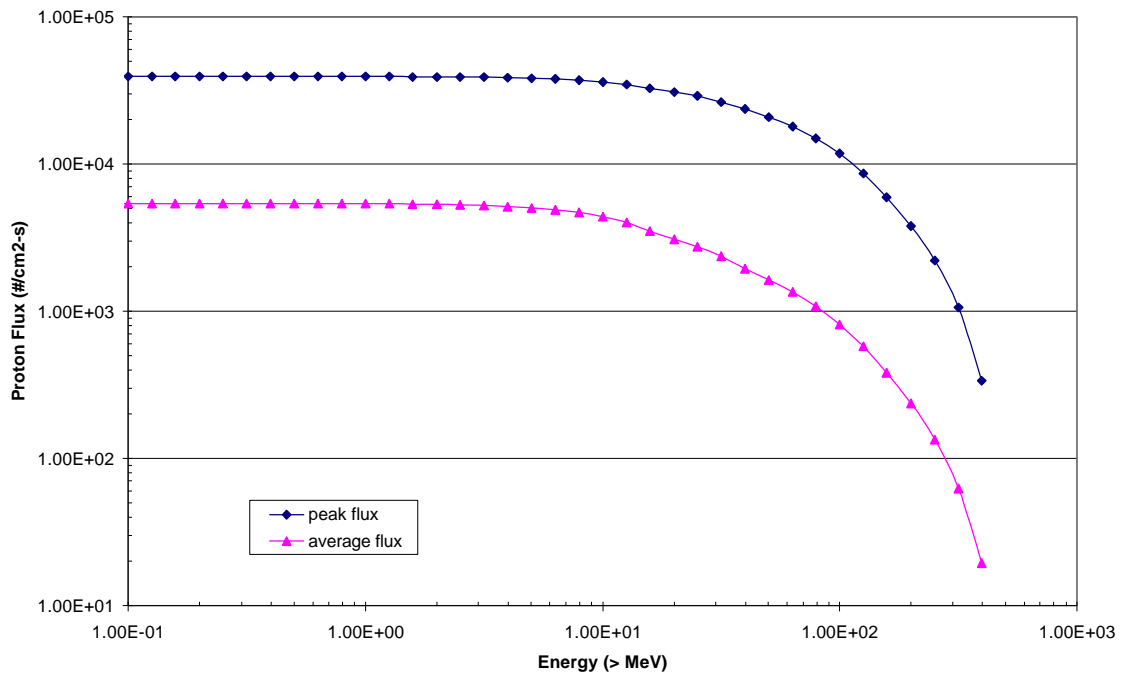


Figure 13: Example of average and peak trapped proton flux spectra.

## 3.2.4 Displacement Damage

### 3.2.4.1 Introduction

In general most of the displacement effect damage in the space radiation environment is due to protons [Mars C 99]. In the particular case of solar cells used on solar panels, the only shielding between the solar cell and the external environment is a thin (as thin as 30  $\mu\text{m}$ ) coverglass coating, and the electron contribution needs to be considered in addition to the proton contribution.

### 3.2.4.2 Determination of the Damage radiation environment for a mission

Generally for a top-level requirement, an arbitrary value of shielding is considered (i.e. 100 mils). When a more accurate analysis is needed, an “equivalent” shielding could be derived from the dose analysis and then the particle spectra could be calculated for this shielding. Otherwise the particle spectra at a specific part location could be calculated with a Monte-Carlo code. Then the DDD or the mission equivalent fluence for a given proton energy is calculated using the Non Ionizing Energy Loss (NIEL) rate [Hopk 96, Mars C 99]. To first order there is a linear relationship between the device degradation from particle induced displacement damage and NIEL for a variety of particles, electrical parameters and devices materials [Mars C 99]. The DDD or the equivalent proton fluence is calculated as follows:

$$\text{DDD} = \sum f(E)N(E)\Delta E$$

$$\text{Mission equivalent proton fluence, } F_D = \sum f(E)N_{E0}(E) \Delta E$$

Where

$f(E)$  is the differential fluence spectrum

$N(E)$  is the NIEL for a particle energy  $E$

$N_{E0}(E)$  is the NIEL for a proton energy  $E$  normalized to the energy  $E0$   
( $N_{E0}(E)=N(E)/N(E0)$ )

$\Delta E$  is the energy step of the sum

Generally only the protons are considered, but if electrons need also to be considered (like in the case of solar cells), the contribution of the different particles is added. NIEL values have been calculated for the following materials: Si, GaAs, InGaAs, and InP. Cheryl Marshall discusses the limitations of the NIEL concept in [Mars C 99]. Generally the NIEL overestimates the displacement damage degradations at high energy, and underestimates the device degradation at low energy.

Figure 14 presents the 10 MeV proton equivalent fluence for a Silicon material for the ST5 mission (elliptical orbit 200-35790 km altitude, 0 degree inclination and three months duration). For this orbit, the maximum contribution of electrons at low shielding is 30% and it is completely negligible after 150 mils of shielding. For the same mission, the electrons dominate the TID environment up to 250 mils of shielding (see Figure 8).

NIEL Proton 10 MeV equivalent fluences  
 ST5: 200-35790 km, 0 degree inclination, 3 months

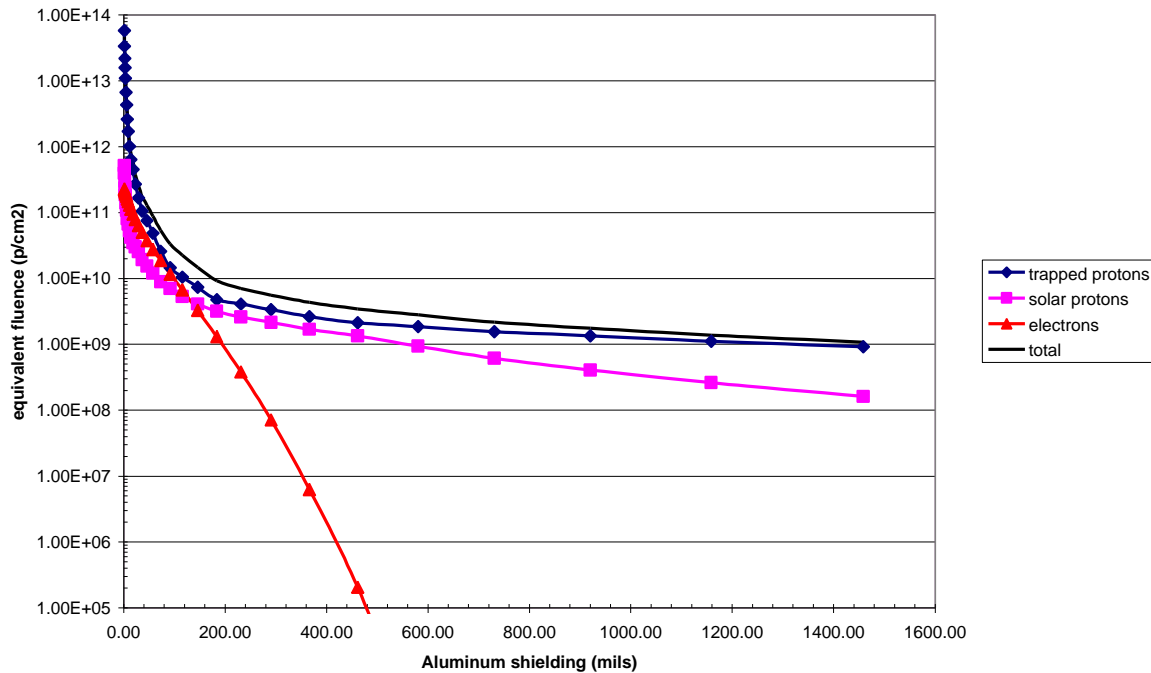


Figure14: NIEL equivalent proton 10 MeV fluence versus Aluminum shielding.

### 3.2.4.3 Solar cell degradation

Calculation of DDD or equivalent fluence based on the NIEL can also be made for solar cells. But generally, engineers use models based on measured damage coefficients: the EQRFRUX-Si and the EQRFRUX-Ga models for Silicon and Gallium Arsenide solar cell degradation calculations, respectively [Tada 82, Ansp 96]. Marvin has also recently measured damage coefficients for multi-junction solar cells [Marv 00]. The solar cells models give a 1 MeV electron or a 10 MeV proton mission equivalent fluence.

These models consider a given thickness of coverglass and assume by default an infinite back-side shielding of cells. But if necessary, a calculation of radiation penetration through the rear-side of solar arrays could be done with a transport code.

## 4.0 BOUND THE PART RESPONSE

### 4.1 Introduction

Knowledge of the radiation sensitive parts is essential to the overall hardness assurance program. However in planning characterization tests, maximum use can be made of part characterizations performed on other programs. Radiation testing is expensive and should be avoided when possible. A careful literature search and analysis can circumvent unnecessary tests. If there is no available radiation data or if the test data is not sufficient, radiation test data must be obtained.

The objectives of radiation testing are threefold:

- Understand the mechanisms of interaction of the radiation with electronic materials and how these effects relate to device failure.
- Characterize the response of specific device types and technologies for use in part selection for specific system application.
- Determine the acceptability of production lots.

These three categories of testing can be considered research, characterization, and hardness assurance. In order to obtain the database needed for these three objectives, the space radiation environment must be simulated in the laboratory. Although attempts are often made to duplicate the space environment to the greatest extent possible by irradiating with the same particle type, energies, and fluxes encountered in space, more often the dominant effect of the radiation is simulated with a convenient radiation source to reduce the cost and technical problems.

For the total dose environment, the damage is caused by the ionization energy absorbed by the sensitive materials, measured in rad. This implies that a number of ionization sources can be used for simulation. However the total dose response is also a strong function of the dose rate.

The single particle environment is usually simulated by the particle LET. For heavy ions this seems to be a reasonable measure of the environment as long as the particle type and energy are adjusted to produce the appropriate range of the ionization track. For protons, however, the LET is not the primary parameter since the upsets result primarily from secondary particles resulting from the interaction of proton with device's atoms. Thus for the proton environment, the simulations must be conducted with protons of the appropriate energy.

Displacement damage can be simulated for any particle by using the value of NIEL. This implies that the effects of the displacement are to a first approximation, only proportional to the total energy loss through displacements and not on the nature of the displacements.

Although the radiation facilities used to simulate the environment are a major factor in radiation testing and are source of large uncertainties [Stas 91], another important factor is the simulation of the operating conditions of the devices. The failure mechanisms of many microelectronic devices exposed to radiation are a strong function of the operating bias, operating mode (standby or active), and temperature. Devices are usually characterized under a variety of test conditions in order to find the worst case operating conditions.

The temperature of many space electronics systems is controlled to be within a range of 0-80°C. Failure levels within this range usually do not vary significantly from room temperature, where most radiation testing is performed. There are some space applications, however, where temperature extremes are encountered, such as cryogenic electronics for certain detectors and high temperatures for some space power systems. In these cases, the failure levels can be significantly different from those measured at room temperature, and the testing must be performed at the appropriate temperature.

## ***4.2 Use of existing Radiation Data***

There are many sources of radiation data on semiconductor devices and microcircuits. Many agencies offer radiation effects databases on the web:

- NASA-GSFC radiation effects data base (<http://radhome.gsfc.nasa.gov/top.htm>)
- NASA-JPL radiation effects data base (<http://radnet.jpl.nasa.gov>)
- DTRA ERRIC radiation effects database (<http://erric.dasiac.com/>)
- ESA radiation effects database (<https://escies.org/>)

The IEEE NSREC data-workshop proceedings, IEEE Transactions on Nuclear Science and RADECS Proceedings are also useful sources of information. Some manufacturers make available the radiation data about their products.

The existence of radiation data on a device does not necessarily indicate the device's acceptability. Most of the available data is either out of date, not well documented (in terms of bias conditions, radiation source characteristics or measurement techniques) or peculiar to nuclear weapons rather than the space environment. For many commercial parts the design is changed, the feature size is shrunk and the process is improved in a continual effort to improve performance, yield and reliability. Many of these changes affect the radiation response.

General guidelines for acceptability of archive data are:

- The tests have been performed with the approved US or European test procedures (see next chapter). For linear devices, if the part has been tested to TID at high dose rate, retesting is recommended.
- A sufficient number of parts has been tested.
- The tested part has the same technology as the part that will be used for flight.
- For TID data, if the lot date code is different, testing is recommended, but may be waived if sufficient process information is gathered. Acceptable conditions for a testing waiver are similar Lot (or date code) with known process changes, or devices for which the die topology and substrate characteristics are known to be the same as for an older lot of devices.
- The electrical parameters/performances important for the application have been tested.
- The bias conditions during testing are worse or equivalent to the application.

The two last steps are perhaps the most difficult. A good example is evaluating test data for SET in linear circuits. In this case, an understanding of what the sensitive SET characteristics (amplitude and duration) are in a design's application is required.

## ***4.3 Testing***

### **4.3.1 Total Dose Testing**

Total dose testing is performed by exposing a device to an ionizing radiation environment and by measuring its electrical performance for a variety of operating conditions. There are two approaches that can be used to characterize the response: step stress and in-flux testing. Step-stress testing is performed by first characterizing the electrical performances

of the device, exposing it to a fixed dose of ionizing radiation, and then measuring again the electrical parameters to determine their change. To determine the device response versus total dose, the test is performed with different samples of the same type at a number of accumulated dose levels. In-flux testing is performed by continually measuring the device response as it is being irradiated. The step stress approach is usually more convenient and much more widely used.

Figure 15 shows the dose rate ranges of the space environment, the different types of irradiation facilities and the recommended ranges in test standards. We can see that the space dose rate is typically lower than  $10^{-3}$  rad/s, and the laboratory dose rates are several orders of magnitude higher.

Generally the ionizing radiation environment is simulated with 1.25 MeV  $\gamma$ -rays ( $\text{Co}^{60}$ ) even though the radiation space environment consists primarily of electrons and protons of various energies.  $\gamma$ -rays give a conservative estimate of the space radiation environment [McLe 87].

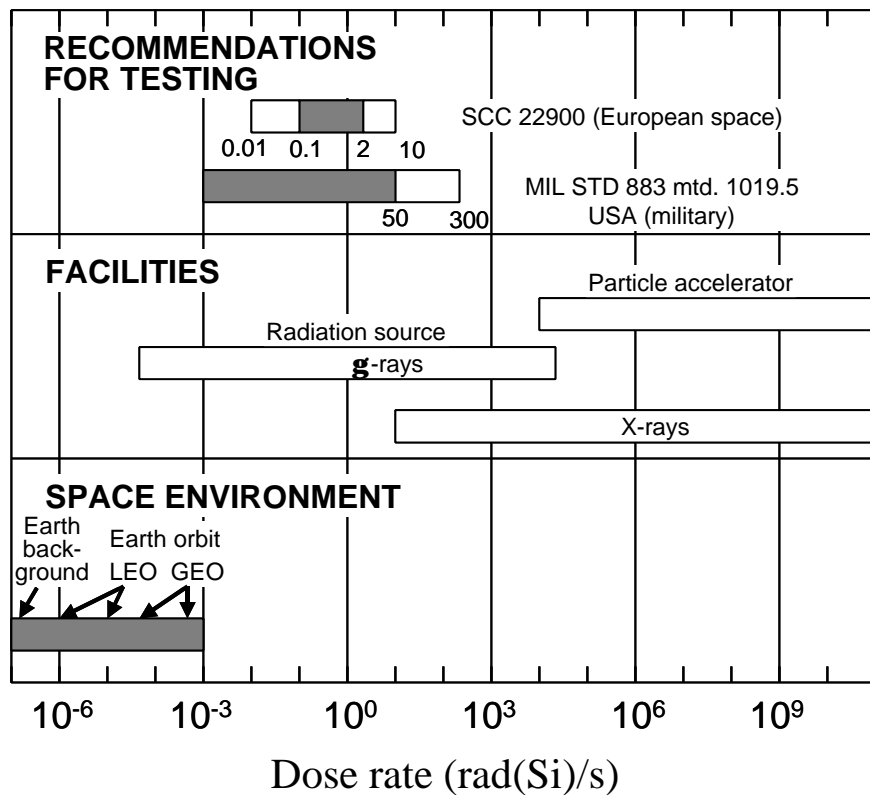


Figure 15: Dose rate and simulation, comparison of the dose rates found in the radiation environments and the rates used in the testing of components for tolerance to cumulative exposure [Holm 93].

Since the parts are used in different conditions in a spacecraft, they are generally biased during testing in the conditions that give the worst-case damage.

Test standards have been developed in the US (MIL-STD 1019.5 and ASTM F1892) and in Europe (ESA/SCC 22900). These standards define the requirements applicable to the irradiation testing of integrated circuits and discrete semiconductors. The MIL-STD 1019.5 procedure was written for military applications and has been adapted for space

applications. The European procedure is only applicable to space applications. Both procedures define the test conditions in order to get a conservative estimate of the part radiation sensitivity of CMOS devices, but in different ways [Wino 93]. There are two areas in which the 1019.5 and the SCC22900 differ. There are first the dose rate, then the dose and the interface trap build-up simulation:

- Dose rate: The standard dose rate window of the MIL-STD 1019.5 (50 to 300 rad/s) is significantly higher than the ones of ESA/SCC22900 (1 to 10 rad/s for the standard window and 0.01 to 0.1 rad/s for the low dose rate window). Both specifications permit the testing at lower dose rates, as long as the dose rate is higher than the dose rate of the intended application. The MILSTD 1019.5 leads to a more conservative measure of the failure dose. However the MIL STD 1019.5 allows room temperature bias anneals following irradiation in order to take advantage of oxide-trapped charge annealing and provide a less conservative measure of the failure dose for the space environment.
- Dose level and interface trap build-up simulation: Both procedures include a one week elevated temperature (100°C) anneal test after the irradiation in order to get a worst case testing of both the trapped holes and interface trap mechanisms, but the details of the test differ. TM1019.5 calls for an additional irradiation to 0.5 times the specification prior to elevated temperature annealing and electrical test. The additional irradiation to 0.5 times the specified dose is required because of the uncertainty in defining worst-case bias during irradiation and anneal. To compensate for this uncertainty, a margin is provided in the form of additional dose. ESA/SCC 22900 does not require an additional irradiation to 0.5 times the specified dose, but instead seeks to accurately identify worst-case bias conditions. TM1019.5 is more conservative due to the overtest. ESA/SCC22900 calls for an additional 24 hours room temperature biased anneal prior to the elevated temperature anneal. This additional anneal contributes in fact a little toward extending the time frame of measurement toward the space application [Wino 93], but it is an allowance to perform irradiation in another location than the testing facility.

Many linear bipolar circuits exhibit enhanced low dose rate sensitivity (ELDRS) [Beau 94, McCl 94, John 94, John 95]. For those circuits MIL-STD1019.5 and ESA/SCC 22900 test procedures may be non-conservative, because the accelerated aging test does not work [Peas 96]. This is why bipolar technology is specifically excluded from the TM1019.5 accelerated aging test. Several accelerated tests for bipolar microcircuits have been suggested. Generally they propose high dose rate irradiation tests at elevated temperature [Witc 97, Peas 96-2, Bono 97], but to date no successful standard test procedure has been found to bound the part response of all types of bipolar linear circuits. For each part type, there is an optimum dose rate and temperature that depends on the dose level. This is illustrated in the example in Figure 16 where the degradation versus dose of the bias current of a LM311 voltage comparator is shown for different dose rate and temperature values. We can see that the 100°C temperature and 5.5 rads/s irradiation condition provides a little enhancement to the high dose rate (28 rad/s) irradiation at room temperature. But the 100°C temperature and 0.55 rad/s irradiation condition gives a very good fit of the low dose rate test (8 mrad/s) up to a dose of 50 krad..

The only approach to take is to perform a low dose rate test. This approach is very time consuming and is generally not compatible with the timeframe of a space project. For example about one year of irradiation at 1 mrad(Si)/s is required to reach a dose level of 30 krad. Fortunately, most low dose rate sensitive parts show a saturation of the enhanced responses at dose rates below a value determined by the most sensitive transistor type for the parameter of interest. For some part types this may be at about 1 rad/s and for others it may be between 1 and 10 mrad/s. The test method ASTM F1892 proposes an approach for the hardness assurance test of bipolar linear devices [Peas 01-2]. The flow diagram is shown in Figure 17. The first step is the review of existing data to determine if the device is sensitive to ELDRS. To date about 25 widely used bipolar linear circuit types have demonstrated low dose rate sensitivity [Peas 96-3, Peas 01-3]. If no data exists an initial test is performed to determine low dose rate sensitivity. It consists in a baseline high dose rate test at room temperature and a low dose rate test (the ASTM F1892 suggests a dose rate at least three orders of magnitude lower than the high dose rate). If the part is not sensitive to ELDRS, the standard TM1019.5 is applicable. If the part is sensitive to ELDRS, two approaches are proposed:

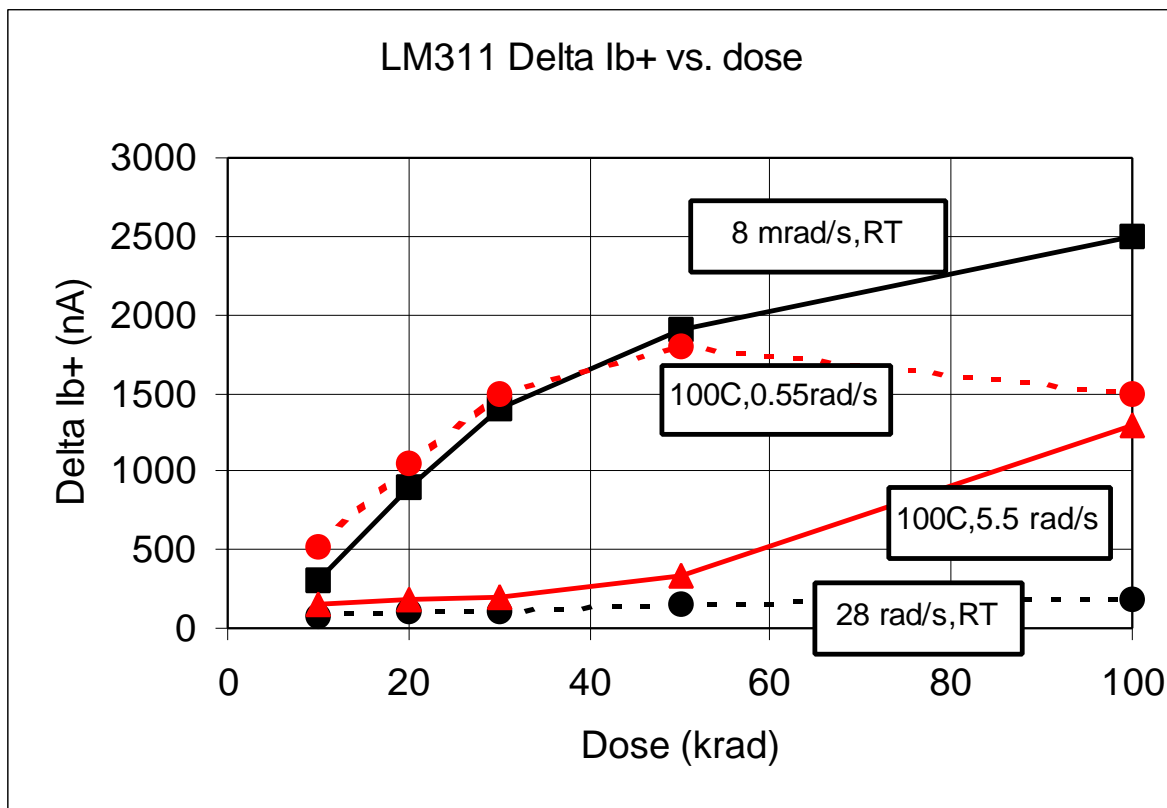


Figure 16: degradation of the bias current versus dose of the LM311 voltage comparator for different values of dose rate and irradiation temperature [Carr 00].

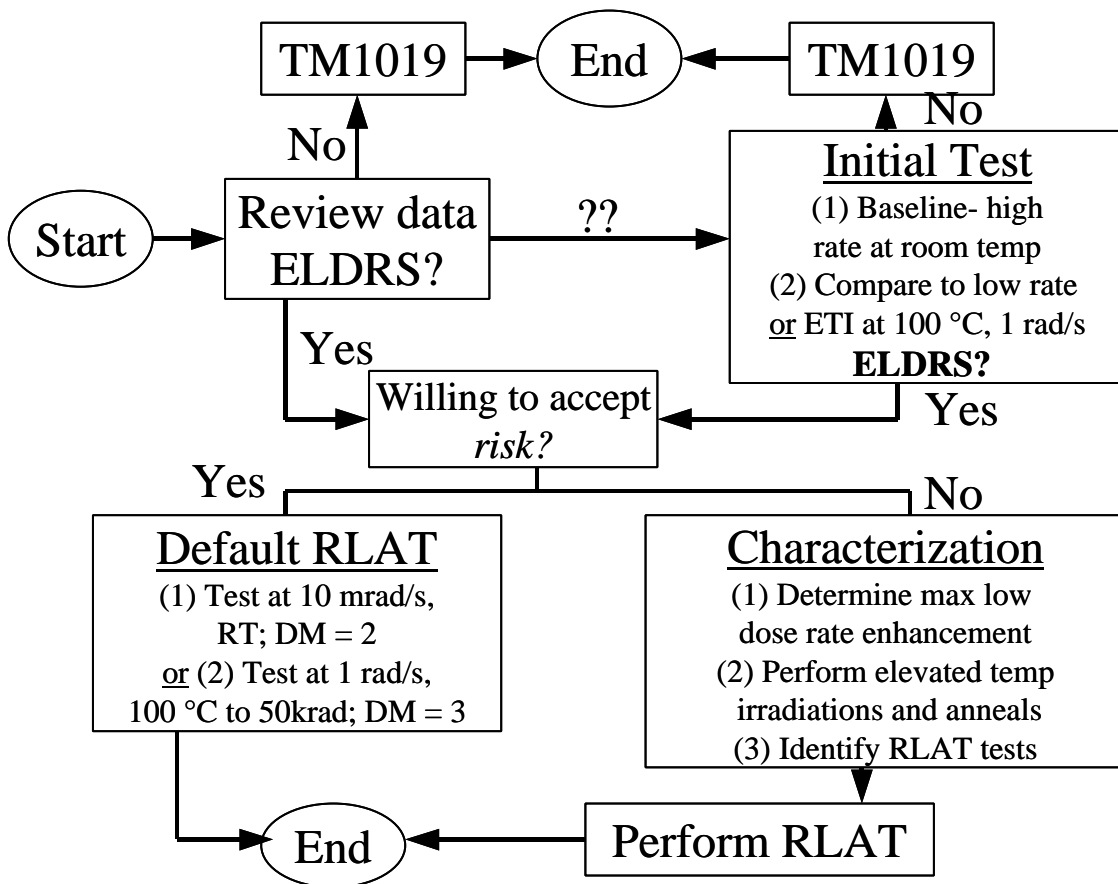


Figure 17: ASTM F1892 ELDRS flow diagram [Peas 01-2]

The first is a pragmatic hardness assurance testing approach using reasonably low dose rates and recommending higher Radiation Design Margins than the ones used for CMOS devices [Peas 98, LaBe 98]:

- Low dose rate at 10 mrad/s with the standard design margin of 2.
- Elevated temperature irradiation at 100°C and a dose rate of about 1rad/s with a design margin of 3 (up to 50 krad).

This approach is simple, but there is a risk of not bounding the low dose rate response of the part with these tests. The second approach is an exhaustive one with many different test conditions to define the adequate test condition for this part.

The ESA/SCC requires a minimum of 11 test samples (10 irradiated parts + 1 reference part). No sample size is indicated in the MIL-STD 1019.5, but the MIL RHA requirements are: 4 parts (0 defect) per wafer in class S and 22 parts (0 defect) per inspection lot in class B. A study performed for the development of the last issue of ESA/SCC 22900 showed that 10 parts are a minimum sampling size for an adequate characterization of commercial parts and bipolar linear devices [Carr 95].

Even a slight variation on the process may have a significant effect on the total dose response. On bipolar linear devices the variation could be important within a single lot and between different lots as illustrated in Figure 21. On COTS devices where there is no information on the process changes, a large variability of the total dose response has been

observed [Peas 96]. For these devices, when there is not a sufficient design margin, it is recommended to test the flight lot.

Other factors have also been shown to have a significant effect on the total dose response: Burn-in [Shan 94], packaging [Clar 95, Dowl 93] and the combination of these two elements. These effects have been studied for several years but are still not completely understood. Therefore the test should be performed not only on parts representative of the flight parts but also with the same packaging and preconditioning.

## **4.3.2 Single Event Effect testing**

### **4.3.2.1 Introduction**

Single Event Effects testing is performed using the in-flux test method. The microcircuit is electrically exercised by a tester and the errors are counted during irradiation.

High energy Galactic Cosmic Rays or Solar Event heavy ions are simulated with low energy ions available in particle accelerators. The index of quality used is the amount of energy lost per unit length of track, the linear energy transfer (LET). As the SEE sensitive regions of many microcircuits are relatively thin (several  $\mu\text{m}$ ), ground testing is conducted using ions with lower energies than GCR or Solar Event heavy ions, but with similar LET. The energy range at the SEE facilities commonly used is of the order of several MeV/u (u is the atomic mass unit) and the penetration range of ions is about from 30  $\mu\text{m}$  for the heaviest particles to 100  $\mu\text{m}$  for the lightest particles. Shortcomings of SEE ground testing have been discussed in several papers [Stas 91, Koga 96, Duze 96, Poiv 01]. Generally the LET concept gives a conservative estimate of part SEE sensitivity. As the range of ions available at ground level is low, these tests are performed under vacuum for low energy beams and the device package in front of the die is removed. At each value of LET the bit error rate is measured by counting a statistically significant number of errors. The SEE cross section in  $\text{cm}^2$  (or  $\text{cm}^2/\text{bit}$ ) is the ratio of the measured number of errors to the ion fluence in  $\text{particle}/\text{cm}^2$ .

To allow a wider range of LET values with fewer ions, it is common practice to adjust the incident angle of the particle beam by rotating the device under test. For a thin sensitive volume with a constant LET through its depth, the path length increases as  $1/\cos\theta$ , where  $\theta$  is the incident angle. This does not change the LET of the ion but increases the path length by the secant of the angle. Thus, as long as these assumptions hold, the “effective LET” increases. Unfortunately this cosine law is not always applicable. It fails in several cases:

- where charge collection occurs over a path length that is a sizable fraction of the total range of the particle (the LET varies along the path),
- for devices that collect much of their charge by diffusion,
- where the aspect ratio of the collection volume is small, causing a more complex angular dependence.

The validity of the cosine law must be carefully checked for each device technology. Test results should always include angle and range data for each ion species. In addition to

these limitations, when the device is rotated, the device package could shadow the ions [Koga 96].

When the effective LET concept is used, the SEE cross section is then calculated as follows:

- effective LET,  $LET(\theta) = LET(0^\circ)/\cos\theta$
- cross section at the  $LET(\theta)$ ,  $\sigma = \text{number of events/fluence} \cdot \cos\theta$

The particle fluence is expressed in particle/cm<sup>2</sup>. The final result of the test is the cross section versus LET curve for each Single Event Phenomenon (SEP).

The energy range of space protons is directly available on synchrotron accelerators at ground level. The testing is similar to the heavy ion test, but for protons it is the SEE cross section versus proton energy curve that is measured. The criterion for proton testing is based on heavy ion threshold LET for the relevant SEP studied. For silicon parts, the proton cross section is negligible when threshold LET as measured using heavy ion is larger than 15 MeVcm<sup>2</sup>/mg; no proton testing is required in this case.

Because proton induced SEPs involve spallation products created after a nuclear reaction between proton and the device's atoms, it is possible to estimate the proton sensitivity based on heavy ion data. Specific models [Roll 90, Pete 92, Douc 95, Calv 96, Miro 98, Bara 00] exist which allow an estimation of the proton induced SEE cross section curves based on heavy ion data. This approach can be used to get a first idea of the device sensitivity, but if this device is critical for the application, a proton testing characterization is recommended.

#### 4.3.2.2 Test standards

Test standards have been developed in the US (JEDEC Test standard 57 or US ASTM F1192-90) and in Europe (ESA/SCC25100). The JEDEC test standard 57 is only valid for heavy ions ( $Z > 2$ ). The ESA/SCC 25100 is applicable for both heavy ions and protons testing. Both methods are similar, the main points are:

- The microcircuits under test shall be delidded for heavy ion SEE testing. This is due to the limited penetration range of the ions available at the ground level. In most of the facilities, irradiation is performed under vacuum for the same reasons. The delidding is generally not required for proton SEE testing and the irradiation is performed in air.
- The ESA/SSC requires heavy ions with sufficient energy to deliver a particle range in Silicon greater than 30  $\mu\text{m}$  (this is not required in the JEDEC 57 procedure). This requirement is important because some modern microcircuits have multiple layers of metallization. In addition charge collection lengths are in the order of 15 to 20  $\mu\text{m}$  for power MOSFETs [Stas 92] and linear devices [Peas 01].
- Both test methods allow the use of the effective LET except for Single Event Burnout (SEB) testing of power MOSFETs. In the JEDEC TM, the maximum tilt angle is limited to 60°.
- Minimum fluence levels:
  - 10<sup>6</sup> ions/cm<sup>2</sup> for soft errors and 10<sup>7</sup> ions/cm<sup>2</sup> for hard errors for heavy ions, 10<sup>10</sup> protons/cm<sup>2</sup> for protons at the threshold.

- Fluence that will induce at least 100 events or  $10^6$  ions/cm<sup>2</sup> ( $10^{10}$  protons/cm<sup>2</sup>) above threshold.
- A minimum of 5 exposures (at different LET or proton energies) is required in order to get an accurate measurement of the cross section curve.
- Monitoring of the dose levels received by the irradiated devices is required. This is particularly important for proton testing where the test fluences are high and therefore the dose levels. It is sometimes necessary to change the parts between the different experimental points.
- The ESA/SCC 25100 test method calls for a sample size greater than 3.
- The JEDEC test standard addresses the specific case of the SEB test of power MOSFET where the response is a function of the drain source voltage (V<sub>ds</sub>) and the LET [Nich 96].

### 4.3.2.3 SEU testing

In the past, single-event testing was relatively straightforward for memory testing. It was generally easy to define the internal conditions and to test the entire storage array of a memory circuit. The test flux just needed to be low enough to avoid complications from multiple errors during short time periods and to correct for the latency period during the time that the memory is being rewritten. But now, large commercial memories use more complex architectures that complicate the testing and make the interpretation of memory test results much more difficult. Now memories are not only sensitive to Multiple Bit Upsets induced by a single particle; they may also be sensitive to large error events [Poiv 00] and also Single Event Functional Interrupt (SEFI) [Koga 01].

Other VLSI devices, such as microprocessors are also very difficult to test. In order to interpret results, one must know which regions of a device involve internal storage cells, and how many of them are being exercised during the test. For example, test results for some types of microprocessors have shown an order of magnitude difference in cross section for different types of test conditions [Howa 01].

The SEE test coverage of the test program and the bias conditions of the part during irradiation play a major role in single-event upset testing. It is important that the test conditions give a worst-case sensitivity compared to the actual application conditions. It is also important to test the part at the application frequency. As feature sizes are reduced with advanced microcircuit technology, the cells become faster, and transients are more likely to be passed as logic signals. A test at lower frequencies may underestimate the device output errors.

### 4.3.2.4 Single Event Latchup (SEL) testing

Many circuit variables affect latchup testing, including the bias conditions applied during testing. Latchup tests should be made under conditions of maximum power supply voltage. Because latchup is a relatively slow process, the diffused charge is extremely important during latchup testing. It is important that particles have a sufficient range.

In most cases a power monitoring and control circuit is used during latchup testing that allows power to be shutdown quickly after latchup is detected. If power cycling occurs,

care must be taken to account for the “dead time” between shutdown and power up when the latchup cross section is evaluated.

Although latchup usually produces large increases in power supply current, some circuits exhibit very small changes in current (“microlatches”). These microlatches may be caused by localized latchup paths, which have relatively high resistance, or by other effects, such as snapback [John 96].

#### **4.3.2.5 Power MOSFETs SEB/Single Event Gate Rupture (SEGR) testing**

The SEB/SEGR testing approach is to identify the threshold voltage  $V_{DS(th)}$  for failure for a given ion, a fixed  $V_{GS}$  and temperature. The selected ion should represent a realistic worst case for the environment. Ni or Fe ions at normal angle of incidence provide a realistic worst case because there is no increased susceptibility from grazing angle ion strikes [Tast 91, Mour 94, Titu 95]. However, it is recommended that these tests be performed at a slightly higher LET with Br or Kr ions.

This approach allows indicating a voltage-operating limit to the designer, but it will not allow estimating the failure probability if the designer chooses to operate above threshold. To obtain SEE rates for a specified environment and operating conditions, a LET cross section curve is needed. In case of SEGR, this approach requires a large sample size and still does not provide an adequate basis for calculating the device failure rate [Nich 96].

#### **4.3.2.6 SET testing of linear analog devices**

One of the characteristics of Single Event Transient (SET) in linear devices is that their pulse widths and amplitude are influenced by the device bias conditions. This makes the SET characterization very complex. A part has to be tested under a large number of bias conditions to get an exhaustive characterization. Another difficulty is that these parts have different sensitive regions that could give totally different transient waveforms. This makes the SET waveform analysis very difficult. It is important to analyze accurately the waveforms because their characteristics will determine the effect of the SET on the application. The test set-up may also have an effect on the transients collected [Poiv 02].

#### **4.3.2.7 Other radiation sources**

Other alternative radiation sources are sometimes used for Single Event studies:

- **Californium:** The fission products from  $^{252}\text{Cf}$  have LET distributed primarily in the range of 41-45  $\text{MeVcm}^2/\text{mg}$  and a range of about 10  $\mu\text{m}$ . Due to this low penetration range  $^{252}\text{Cf}$  could only be used to get a qualitative estimate of SEE sensitivity. This test is useful to check the test set-up before accelerator testing and is a cheap way to compare SEP sensitivities for part type preselection.
- **Laser:** Laser light is also an easy way to create SEEs in devices in the laboratory. This technique has been proved to be very useful for SEE mechanism studies and part hardening [Buch 96, Poug 00]. It can also be used

for part assurance screening to compare the sensitivity of different manufacturing lots. But laser light and heavy ion charge deposition processes are fundamentally different. So laser testing cannot be used directly to characterize the in orbit behavior of a part. Heavy ion test data is always necessary to calibrate the laser data on a given part.

### **4.3.3 Bulk damage, displacement effect testing**

Displacement damage testing for the space environment is performed using the step stress approach. Although a significant amount of transient annealing can occur immediately after a short pulse of radiation, this effect is not a factor for space particle fluxes. The permanent damage is stable at room temperature, hence no significant annealing occurs between irradiation steps.

It has also been shown that bias has little effect on the permanent displacement damage. This allows irradiation to be performed passively [Mars C 99]. Therefore displacement damage testing consists of simply characterizing the electrical performance of the part, exposing to an irradiation source, without bias, to a fixed particle fluence and characterizing it after irradiation to determine the parameter degradation. However, for photonics devices the degradation may be application dependant. For example, Reed showed this application dependence for optocouplers in [Reed 98]. For these devices active measurements, that match the application, are recommended.

The radiation source used is generally a mono-energetic proton beam, and the part is irradiated to a fluence greater than the mission DDD or equivalent fluence established with the NIEL. It is very important to choose adequately the test energy. For low quantities of shielding a low energy (ie 10 MeV) is adequate because it represents best the environment. For higher shielding, a higher energy is needed (ie 60 MeV), because most of the damage results from protons higher than 10 MeV [Mars C 99]. Reed recommends testing optocouplers at multiple energies because of the inconsistency between experimental determination of damage factors and theoretical calculations with NIEL [Reed 02].

Protons are also heavily ionizing with a larger fraction of the energy loss going into ionization, therefore the effects will include both displacement and ionizing dose damages. The test total deposited dose needs to be calculated and the results compared to a Co-60 TID test to sort out failure mechanisms.

For solar cells the radiation source is generally a mono-energetic electron (1MeV is a standard value) or proton (10 MeV is a standard value) beam, and the part is irradiated to a fluence greater than the mission equivalent fluence established with the NIEL or with the damage equivalent models.

## **5.0 DEFINE THE SYSTEM/SUBSYSTEM RESPONSE TO THE RADIATION ENVIRONMENT- PARTS CATEGORIZATION**

### ***5.1 General***

Considering the individual part radiation sensitivities, the radiation environment and the system/subsystem design, an analysis of the system/subsystem response is performed. For each radiation sensitive part the Radiation Design Margin (RDM) is defined and then each part could be classified as Hardness non critical, Hardness critical or not acceptable. For the parts belonging to the two last categories, risk reduction actions are taken.

### ***5.2 Total ionizing dose***

#### **5.2.1 Define the radiation failure level**

The radiation failure level of each part in each application is defined. This corresponds to the maximum parametric and functional device characteristics limits so that the application/function will operate according to specification over the design lifetime. This is a two step process: first the maximum parameter limits are defined via circuit analysis, then the part radiation data is used to define the radiation failure level  $R_f$ . As, the distribution of failure levels follows often a lognormal law, Pease recommends that the geometric mean  $R_{mf}$  be used to represent the nominal value of the failure level  $R_f$  [Peas 94].

The design radiation analysis is part of the design Worst Case Analysis (WCA) that combines the effects of radiation, temperature and parts aging. Circuit WCA is needed on each engineering subsystem and science instrument in order to demonstrate that the design will work in its environment under the most stressful operating conditions (data rates, voltages, switching transients,...). The circuit WCA is usually performed by the design engineer.

Figure 18 shows the degradation of the offset voltage  $V_{io}$  of an operational amplifier PM155 versus total dose. The data has been collected on 8 parts from the same lot and the average has been calculated. If we consider the specification limit of 2mV, the failure level  $R_f$  is about 40 krad. If we consider an acceptable limit for a given design of 4 mV (this means that the acceptable  $V_{io}$  for this design will be higher taking into account the temperature variation and the part aging),  $R_f$  will be about 75 krad for this particular application.

## PM155

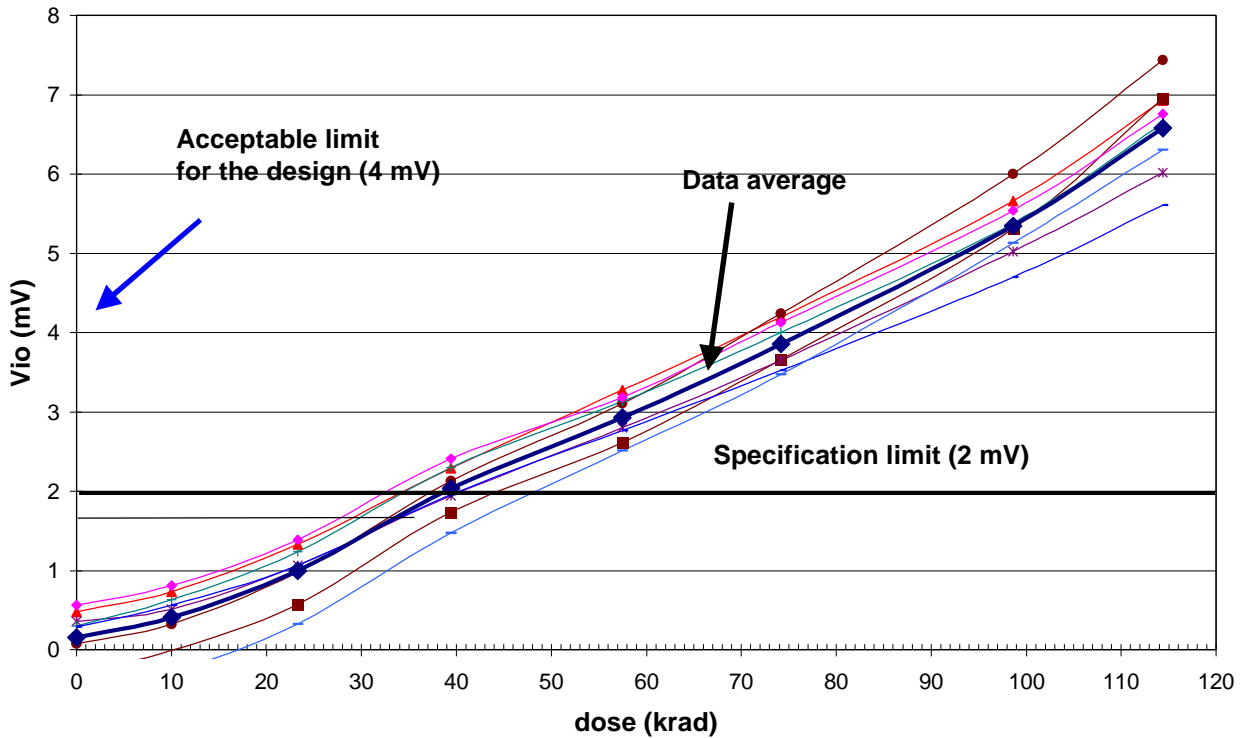


Figure 18: degradation of the offset voltage of a PM155 operational amplifier versus total dose.

## 5.2.2 Define the radiation specification/levels

### 5.2.2.1 Introduction

The radiation levels for each sensitive part are defined by the methods described in chapter 3. For a given part type, the radiation level is defined as the worst-case radiation level. Generally the power budget and weight are critical parameters for a space system. Because of the ease of stopping some part of space radiation, all components of a spacecraft can be thought of as shielding one another. All mass surrounding a radiation sensitive part can be regarded as shielding or protection even though that mass serves other primary, usually structural, purposes. Electronic box platforms, box covers and circuit boards also provide shielding. A part in the center of a stack of printed circuit boards may be exposed to only one tenth of the dose received by the same circuits on the uppermost board of a stack. The spacecraft and electronic boxes layout has a fundamental importance in the design of a radiation tolerant spacecraft. Therefore, an accurate model of the spacecraft and a radiation analysis will allow defining the lowest radiation levels.

### 5.2.2.2 Spacecraft materials

A space vehicle is composed of a large number of small components of widely varying materials. Generally it is impractical to consider every material in the dose analysis, and

generally we consider an “equivalent thickness” of a representative atomic number like Aluminum.

But if the analysis is performed with a Monte Carlo code, it will be much more accurate to consider the real nature of the materials.

### 5.2.2.3 Spacecraft structure as a radiation stopper

To calculate the dose levels at a given point within a given box, all radiation-absorbing masses present in the satellite have to be taken into account. These, of course, constitute an extremely complex array of masses, but an accurate model will allow one to calculate as closely as possible how they contribute to radiation stopping [Holm 93]. The dose analysis could be done by a sector analysis or a Monte Carlo simulation as described in chapter 3.2.2. Figure 19 shows the results of a Monte Carlo radiation analysis performed on different locations within the electronic box of the ST5 spacecraft. These results illustrate the significant effect of a location within a spacecraft. If the radiation shielding is considered when the spacecraft layout is defined, a significant shielding can be provided without any added weight to the most sensitive parts. In the ST5 example, it has been decided at the beginning of the project to put the Command and Data Handling (C&DH) subsystem in an enclosure at the center of the spacecraft. We can see in Figure 19 that the dose levels for the different points analyzed in the C&DH subsystem are lower than 5 krad. This allows the use of commercial memories in this subsystem.

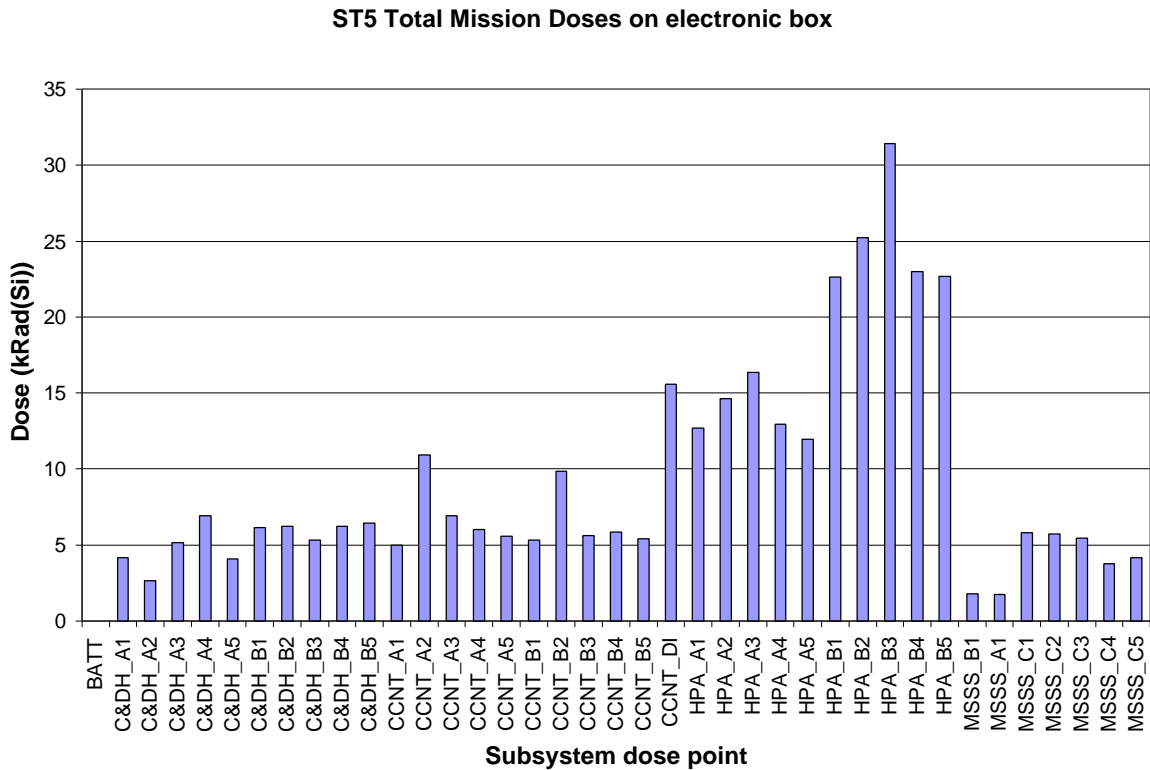


Figure 19-a: ST5, dose levels within the spacecraft.

### ST5 Total Mission Doses on electronic box

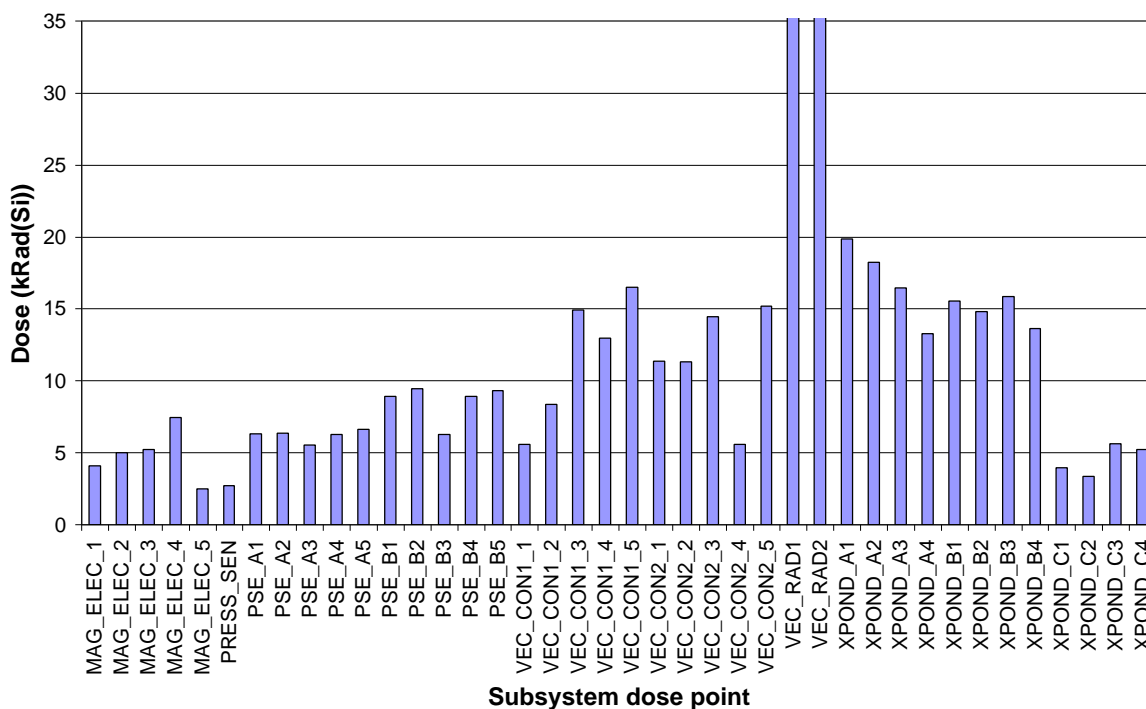


Figure 19-b: ST5, dose levels within the spacecraft.

#### 5.2.2.4 Add-on shielding

If built in mass on the spacecraft cannot be arranged so as to protect all sensitive components, then-as a last resort-some ‘add-on’ absorber may have to be judiciously added. The first aim of add-on shielding is to interpose a few millimeters of any suitable material between the device of interest and the external environment. If the array of devices to be shielded is small, we can save weight by enclosing the array in a compact shield rather than build the same thickness outside the box. This is the idea of local shielding: simply to obtain a given dose reduction in a given volume for the minimum weight penalty. For instance, a single integrated circuit would be best protected by a blob of filled plastic applied directly to the package or by using heavier materials (like Kovar, Tantalum,..). This type of shield is called a spot shield.

The particle-scattering property of materials has some dependence on the atomic weight. This is weak in the case of protons and strong in the case of electrons. Thus the choices of atomic weight for an add-on shield in a proton-dominated orbit might differ from that for an electron-dominated orbit such as the geostationary case [Mang 96]. Heavy materials like Tantalum and Kovar have a better shielding efficiency for electron-dominated environments. A better shielding efficiency means that the same shielding will be provided for less weight of shielding material. Light materials like Aluminum oxide ( $Al_2O_3$ ) have a better shielding efficiency for proton-dominated environment. However the effect of the material is not very significant (less than 10%) in these orbits [Astr 01].

Some “hardened packages” made with layers of heavy and light materials could be a very effective way of protecting a sensitive device, especially in the case of electron dominated orbits. But, a spot shield of about 1 g/cm<sup>2</sup> on a standard package will have a similar effect [Astr 01].

### 5.2.3 Parts categorization

Once the radiation specification levels and part failure levels are determined for each part type, the categorization criteria are applied to determine the suitability of the part. The categorization criterion is based on the Radiation Design Margin (RDM) defined as the part failure level  $R_f$  divided by the radiation level  $R_l$ . The uncertainties in the environment, part tolerance and shielding analysis are considered in the design margin. The US Space Working Group (SPWG) has developed two formalisms for categorization: the Design Margin Breakpoint (DMBP) and the Part Categorization Criterion (PCC) [Peas 94]. The DMBP is a qualitative approach recommended for systems with moderate requirements according to the guideline document for ionizing dose and neutron hardness assurance MIL-HDBK 814. The application of the DMBP method for categorization is shown in Table 5.

Table 5: Application of the DMBP method for categorization [Peas 94].

<b>RDM</b>	<b>Categorization</b>
< 1-2	Unacceptable
1-2<RDM<10-100	Hardness Critical
RDM>10-100	Hardness non critical

If a part is found to be unacceptable, the alternatives are:

- expertise and radiation analysis: perform a more accurate analysis of the received radiation levels to determine if the expected dose levels are actually lower. Test the part in the application conditions, or at low dose rate (CMOS device) in order to increase the part radiation failure level.
- Redesign the system either to change the part failure level (design hardening) or to change the dose level (change the spacecraft layout, spot shielding).
- Substitute a harder part.

Acceptable parts may or may not require hardness assurance. The dividing line between whether or not hardness assurance techniques are required is usually set at an RDM of 10-100 [Peas 94]. Parts that are categorized as hardness non-critical could be used with no further evaluation. For those devices which are hardness critical, the most used hardness assurance testing is the flight lot sample radiation testing.

The PCC method is a more quantitative approach to part categorization. In this method a statistical approach is used based on an average and standard deviation of the sample characterization data [Peas 94]. PCC is defined as:

$$PCC = \exp(K_{TLS}) \text{ for log normal distribution law}$$

or

$$PCC = 1 + K_{TLS}/R_l \text{ for a normal distribution law}$$

where

$$s = \text{standard deviation of the radiation test data}$$

$K_{TL}$  = one sided tolerance factor based on sample size  $n$ , confidence level  $C$  and probability of survival  $P_s$ .

To apply the PCC approach to categorization, one may first define a probability of survival and a confidence level for the system or subsystem considered, then, a  $P_s$  and  $C$  could be established for each part. The values for  $K_{TL}$  are given in the MIL HDBK-814. Figure 20 shows the values of the one sided tolerance factor in function of the test sample size for some values of  $P_s$  for a 90% confidence level.

We can see in the figure that  $K_{TL}$  increases very quickly for sample sizes lower than 10, smaller values of  $n$  will give high values of PCC. The application of the PCC method for categorization is shown in Table 6.

Table 6: Application of the DMBP method for categorization [Pease 94].

RDM	Categorization
$< 1-2$	Unacceptable
$1-2 < RDM < PCC$	Hardness Critical
$RDM > PCC$	Hardness non critical

Figure 21 shows the degradation versus dose of the bias current  $I_b$  of a PM155 operational amplifier. 22 samples from three different manufacturing lots have been used. The average and the one sided tolerance limit have been calculated based on log normal law,  $P_s=99$  and  $C=90\%$ . For these values of  $P_s$  and  $C$ ,  $K_{TL}$  is equal to three.

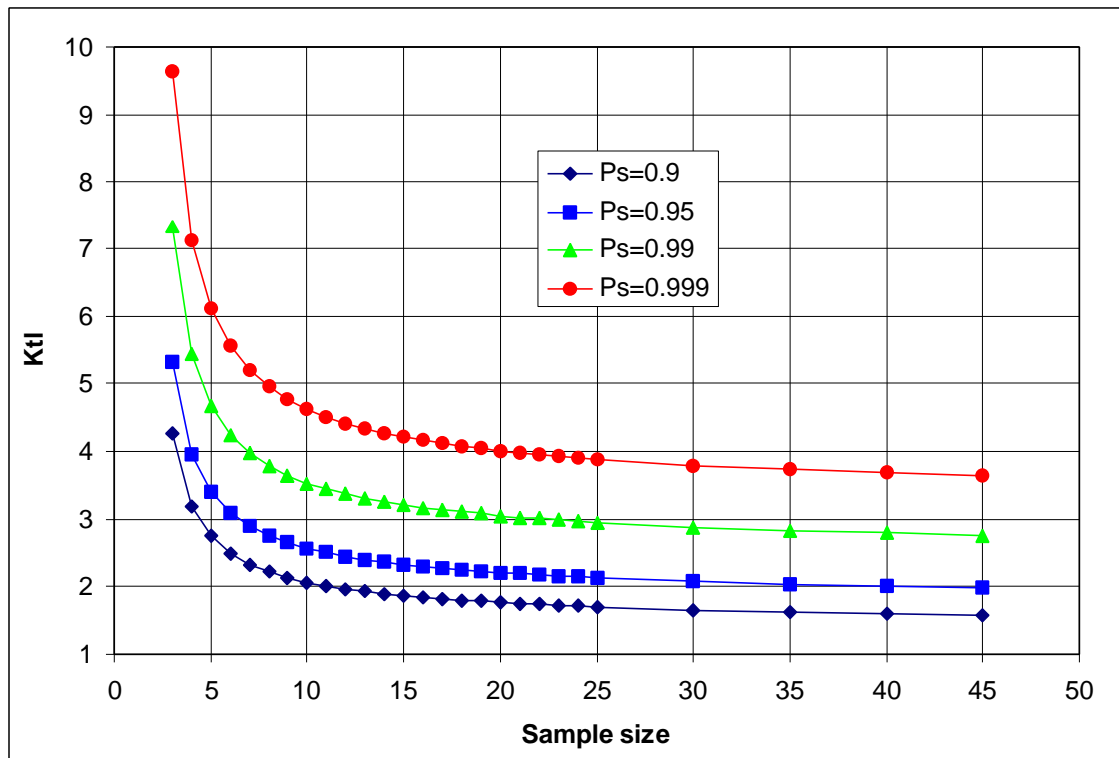


Figure20: Values of  $K_{TL}$  in function of  $n$  and  $P_s$  for  $C=90\%$ .

## PM155

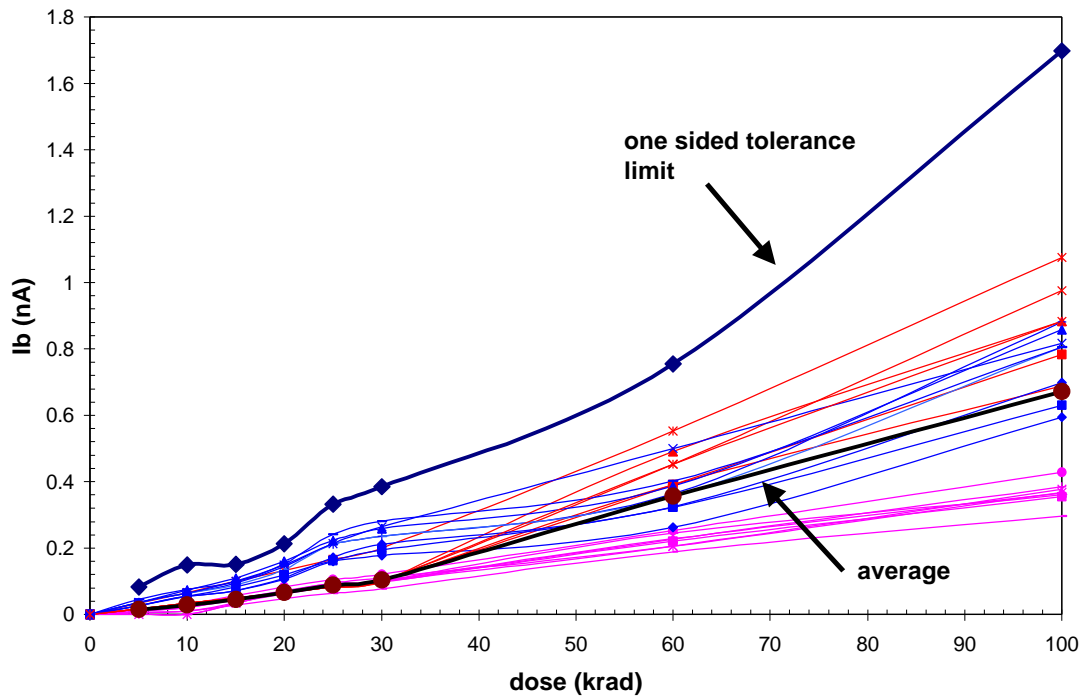


Figure 21: Degradation versus dose of the bias current of a PM155 operational amplifier.

If the maximum current is 0.4 mA, the failure level, based on the average, Rmf is equal to about 66 krad. If the radiation margin is equal to 1, 50% of the parts will fail this criterion. This risk is generally unacceptable. If the dose level is 33 krad, the RDM is equal to 2, and is close to PCC. Therefore, the risk of failure will only be 1% with a confidence level of 90%.

### 5.3 Displacement Damage

The approach for displacement damage analysis is similar to TID. The test data and the design WCA allow the definition of the failure level  $R_f$ . Then, the failure level is compared to the DDD or the mission equivalent fluence to define the Radiation Design Margin. Generally the design margins requirements for DDD and TID are the same.

Devices sensitive to Displacement Damage are also sensitive to TID. For proton dominated space environments, DDD proton testing can deliver sufficient TID to estimate both the DDD and TID induced degradation. Otherwise, the effects of TID and DDD need to be combined for the design WCA. Reed proposes such an approach to estimate the CTR degradation for a specific mission DDD and TID [Reed 01]. The process is shown in Figure 22.

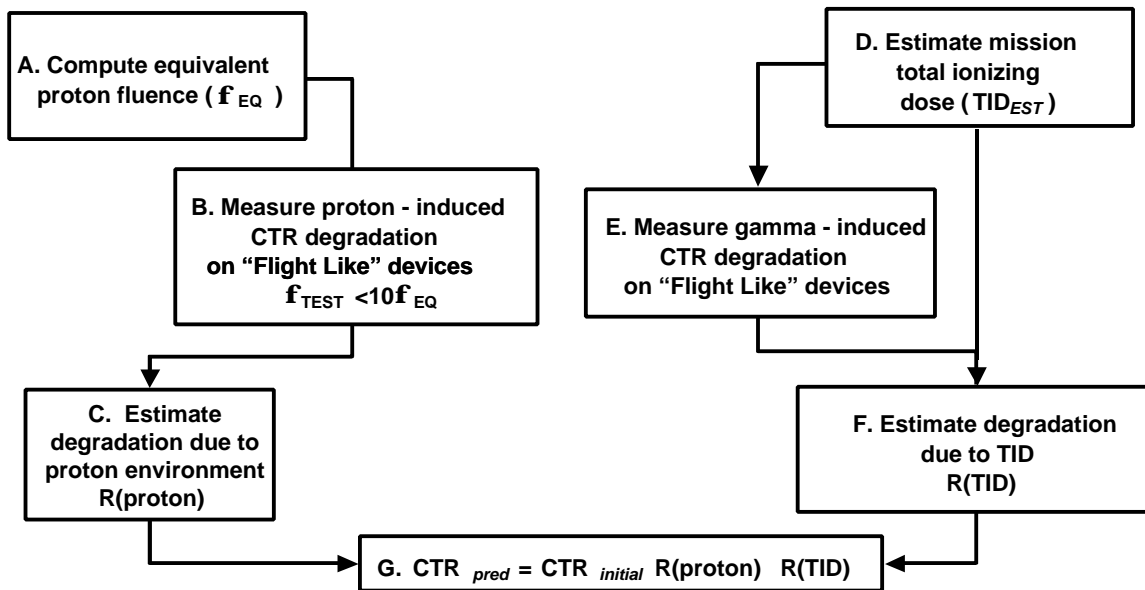


Figure 22: Process for estimating CTR degradation of optocouplers [Reed 01].

## 5.4 Single Event Effects

### 5.4.1 General

For SEE analysis, the SEE data is compared first to the radiation environment and then a Single Event Effect Criticality Analysis (SEECA) is performed. Different approaches to SEE analysis depend on the possibility of calculating a SEE rate.

### 5.4.2 Error rate Prediction

When SEE error rate predictions are technically possible (case of Single Event Upset, Single Event Latch-up, Single Event Transients, for example), an error rate is calculated based on test data and the SEE radiation environment. Table 7 shows an example of analysis requirements depending on the part SEE sensitivity. Heavy ion and proton induced SEE rates will be calculated under quiet and under solar event conditions.

Table 7: Example of SEE analysis requirement.

SEE LET threshold	Requirement
$> 100 \text{ MeVcm}^2/\text{mg}$	SEE risk negligible, no further analysis needed
$15 \text{ MeVcm}^2/\text{mg} < \text{LETth} < 100 \text{ MeVcm}^2/\text{mg}$	SEE risk low, heavy ion induced SEE rates to be analyzed
$\text{LETth} < 15 \text{ MeVcm}^2/\text{mg}$	SEE risk high, heavy ion and proton induced SEE rates to be analyzed

Calculation of heavy ion SEE rates involves three different quantities:

- The cross section curve of the device determined experimentally
- The heavy ion LET spectra and proton energy spectra
- The critical charge, sensitive area and sensitive volume associated with the SEE of interest.

The sensitive geometry and critical charge are the most difficult parameters to determine. Charge funneling, which extends the collection depth below the depletion region, cannot be determined directly and involves an assumption about device geometry. Charge collection assumptions are more straightforward for epitaxial processes, where it is usually reasonable to assume that the charge collection depth is limited by the epitaxial layer thickness [John 96].

CREME96 is the standard tool to calculate the SEE rates with the help of HUP and PUP routines for heavy ion induced SEE and proton induced SEE respectively. The HUP routine uses the standard Integral Rectangular Parallelepiped (IRPP) method to calculate the Single Event Effect rate [Pick 96]. Either the test data or a Weibull fit of the test data could be used. The proton induced prediction method is a direct convolution of the proton energy spectrum with the upset cross section versus energy curve. Either the two parameter Bendel model or a Weibull fit (if there are sufficient data points) could be used to define the proton test data.

Some optoelectronics devices (photodetectors, fast optocouplers) are also sensitive to proton induced direct ionization. Single Event rate prediction methodologies have been proposed [Reed 01, Mars P 02]. They generally use the standard tools available in CREME96. These techniques are still under validation.

### **5.4.3 Criticality analysis**

#### **5.4.3.1 Introduction**

SEE requirements depend on the functions the devices perform. Many SEEs are different for different device types. For example, memories will exhibit different conditions than linear devices. In addition, SEEs may present functional impacts by propagating through the design and impacting other areas. These two conditions make each single event problem different in terms of failure mode and effect. SEE analysis is most effectively supported by viewing a design or system from the perspective of the function(s) performed.

The objective of a conventional functional analysis is to define a comprehensive set of baseline functions and functional performance requirements which must be met in order to accomplish the overall mission objectives. This is achieved by the breakdown of top-level requirements into successively lower level performance requirements, in a methodical and traceable manner. Functional analysis applied at lower levels involves the breakdown of requirements and functions at the subsystem, card, circuit, and device levels. Top-level functional analysis is useful in requirements generation, such as for SEE tolerance. Lower level functional analysis is useful in SEE impact assessment, or failure modes and effects analysis.

One objective of viewing a design or system in terms of function is to determine the criticality of the function(s) performed on an operational level. Many SEEs present a functional impact, but do not cause permanent damage to the device. Depending on the criticality of a function, these non-destructive conditions may or may not be acceptable in

a design. In assessing criticality, we determine the impact of an SEE in a device on the functions it performs. Device hardness requirements are not considered here, since SEEs may be mitigated through many routes. What is of interest is the operational impact of a specific device SEE propagating through the design or system.

Functions may be categorized into “criticality classes” or categories of differing severity of SEE occurrence. Many times, most or all of the functions performed by a design or system are considered critical to a mission. The operational impact of SEEs in critical functions may be unacceptable. For these designs, usually either no single event effects, or a very small probability of SEE occurrences, are permitted. When considering a subsystem, some components may not be SEE-critical, while data storage memories may tolerate SEEs if utilizing error correction schemes. Both of these functions are located in the Data System.

In general, one might consider three criticality groups for Single Event Upset: error-functional, error-vulnerable, and error-critical. Functions in the error-functional groups may be unaffected by SEUs, whether this immunity is due to an implemented error-correction scheme or redundancy, and a large probability of SEU at the device level may be acceptable. Functions in the error-vulnerable group might be those for which the risk of a low probability is acceptable. Functions in the error-critical group are functions where SEU is unacceptable. Figure 23 shows the decision tree for criticality analysis.

This functional criticality concept applies directly at the device level. One may specify the criticality of a device function and determine whether current device tolerance needs and mitigation schemes are adequate to protect the system from impacts. Functional criticality is also a direct lead into SEE requirements generation on any level, including spacecraft, system, and subsystem.

Once the criticality of functions is determined, requirements for design, including hardware and software may be directly obtained. The more critical a SEE is to operational performance, the stricter the SEE requirement should be. Figure 24 shows the SEE requirement generation flow.

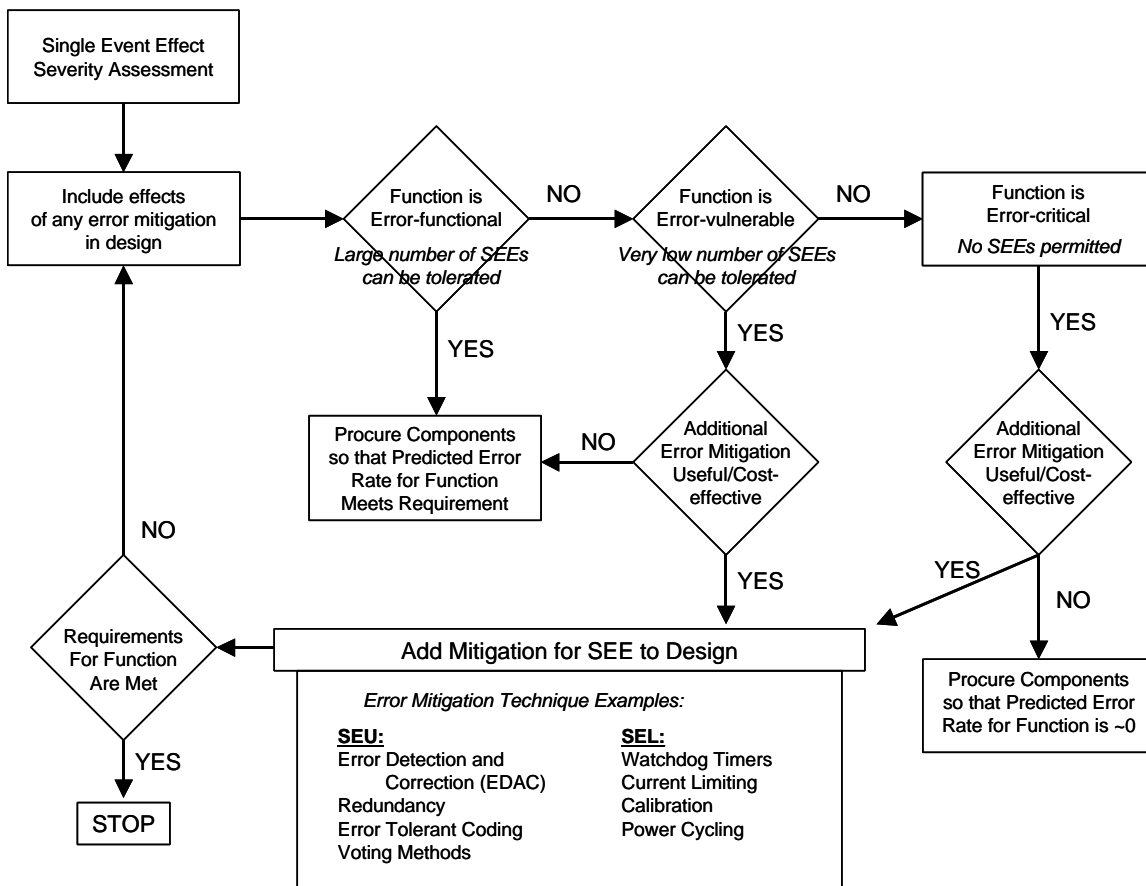


Figure 23: Decision tree for criticality analysis.

### 5.4.3.2 SEU propagation [LaBe 96]

A SEU that appears at a device output propagates to its associated circuitry and the analysis of the impact of this upset at subsystem, system and spacecraft level should be performed. For example, a SEU that occurs in an Analog to Digital converter can cause a single incorrect data sample to be gathered. This “invalid” data sample may provide an incorrect data point such as a star location or a misleading telemetry value.

The concept of propagated SEUs is straightforward to the typical electrical engineer. It is similar to what one might perform in a standard circuit simulation, that is, how a signal pulse, transient, or state will affect a circuit’s performance instantly or in future clock cycles. SEU propagation analysis is also similar to Failure Mechanism Analysis (FMEA). In both instances, the end goal is to determine the end effects that an error or failure has on performance of a device, circuit, or system.

The first step is to determine where and what type of SEU may occur. How a device is being utilized in its specific application may affect its SEU performance as well. Parameters such as access rates, operational modes, clock frequency, power supply voltage, etc., have definitive impacts not only on the occurrence, but also on the observed effect of an SEU. For example, on an LM139 voltage comparator, most of the transients have a large amplitude when the differential input voltage is low.

Now that we have determined the sensitive devices and operational effects on observed SEUs, the determination of what apparent effect the SEU has on device performance must be explored. Several outcomes may appear. These include, but are far from limited to:

- improper device operation
- incorrect device output
- errors in memory structures to be accessed externally
- noise spikes on transmission lines
- device mode change such as going from an active to standby mode, functional interrupt
- incorrect device timing

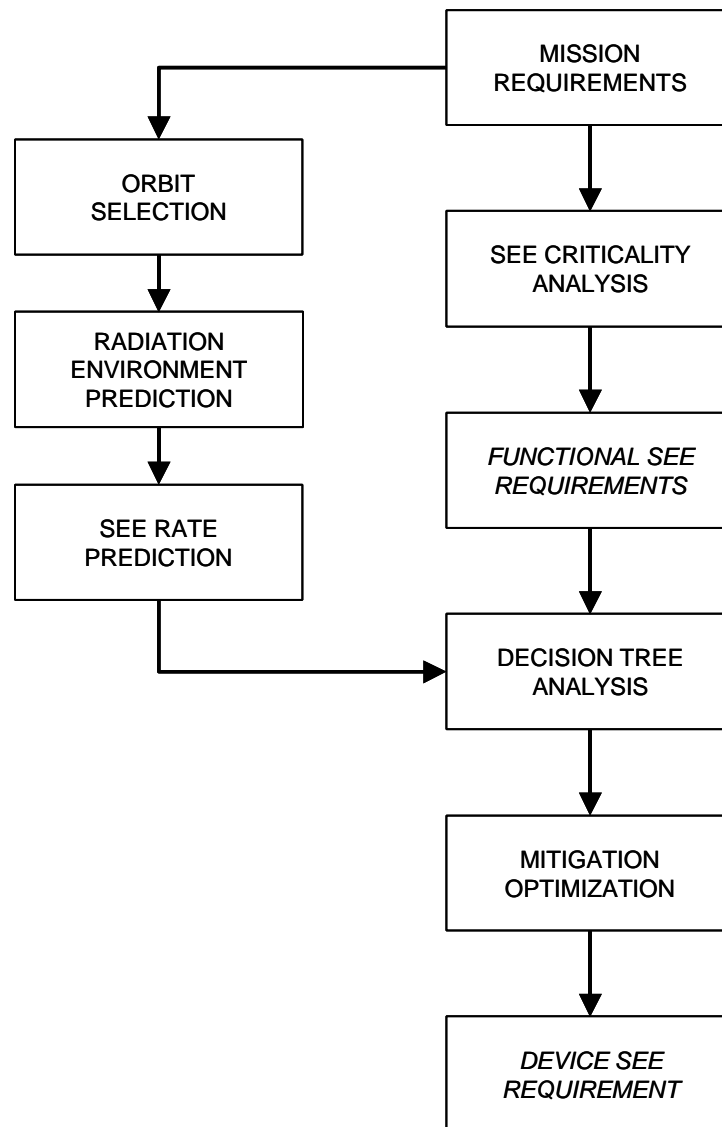


Figure 24: SEE requirement generation flow chart.

Circuit level analysis follows the same steps but with the key now being the circuit operation and performance. As with device level analysis, once we know which devices have SEUs and what those SEUs may look like, we then look at the operational parameters and their impacts on SEU performance. For example, we know that a bit flip

may occur in a SRAM, but the circuit level effects are dependent on the way the SRAM is being used for in this application. Sample propagated effects might include:

- an SEU in a SRAM being used for data storage: a bad data point.
- an SEU in a SRAM holding software program instructions: improper operation or flow.

Once the operational analysis is performed, the engineer is again able to perform a circuit simulation using digital or analog tools. The output of this analysis is a list of the potential SEUs in a circuit and their effects on circuit operation. We may view this as a “black box” wherein the internal circuitry doesn’t matter, but what is observed by the outside world (subsystem, system) is noted.

We may treat subsystem, system, and spacecraft levels of analysis in a similar manner. Once the circuit level analysis is complete, we begin the subsystem level analysis. In essence, we may treat the subsystem exactly like the circuit level, but look for performance aspects of the SEU-induced anomaly. The system level takes this one step further. The spacecraft level of analysis then would take the output of the system level analysis and determine, in this case, whether the incorrect command would affect the overall spacecraft operation. For example, we might observe incorrect instrument data being gathered or a system safing occurrence.

An example of this type of analysis is given in [LaBe 96].

### 5.4.3.3 Definition of SEE requirements [Mars P 96]

#### 5.4.3.3.1 System level requirements:

The system level requirements should be expressed in view of all possible ways in which Single Event Effects could compromise mission performances. The two main categories are system availability and information quality.

- **System availability:** System availability requirements address extreme events leading to possible loss of mission as well as less severe events which might require ground station or possibly autonomous reset with a brief disruption in system performance. Typically, availability requirements for Single Event Effects have been expressed in general terms along the lines of “no single event effect (e.g., latch-up or any other potentially catastrophic SEE related failure mode) shall be allowed to result in the loss of the mission.” Additional availability requirements can be specified in terms of the severity of disruption, the acceptable frequency of disruption, or the maximum duration of disruption, or some combination of the three. In addition to SEE induced hard failures, soft errors may occur which disrupt system performances but allow complete system recovery. For example, it might be required that the normal mission operations not be disrupted by any single event effect with an outage requiring ground station intervention more than once per year, and the occurrences of autonomously reset disruptions cannot happen more than once daily with the system recovery required to result in an overall system availability of 0.9993 (corresponding to system unavailable for 1 minute per day on average). SEE requirements might

also reflect the compromise between mission objectives and cost constraints by allowing for less stringent performance under extreme circumstances. For example, if the mission science objectives of a LEO platform do not require highest availability levels while in the South Atlantic Anomaly (SAA), then the SEE/SEU requirements might be relaxed in that region with substantial cost savings. Similarly, if more frequent disruptions of operations could be tolerated for short duration over the course of a multi-year mission, then the requirements could be relaxed for anticipated solar flare related particle bombardment, which might be several orders of magnitude more harsh than daily peak particle fluxes under normal conditions.

- **Information integrity:** As a separate requirement from system or subsystem availability, the mission might consider the payload functional requirements in term of information integrity. In many cases, soft errors can occur in a relatively benign manner which affect data without altering the system functions. For example, a soft error in a sensor A/D converter or in a data path might result in a glitch in an image. Such errors do not interrupt the flow of information, but rather degrade its quality. These less severe types of single event errors lend themselves to Error Detection and Correction (EDAC) techniques [LaBe 96]. The implementation of EDAC and the type of approach selected should be based on the following: the environment, the hardware, and the requirements for data integrity. The establishment of reasonable requirements at the mission planning stage should lead to acceptable, but not necessarily error free, performance within constraints of cost and design complexity. The form of the data integrity requirement for the payload will likely reflect the type of information being collected and how it is handled between collection and downlink. As an example, a charged coupled device (CCD) for earth imaging might be the source of a data stream which flows from a camera through a data bus to a solid state recorder and then to a downlink. In such a case the top level requirement might be, for example, no more than 3 bad pixels per frame of imagery. Another form of a top level requirement in this example might be a bit error rate (BER) requirement. The establishment of such top level requirements provide the basis for subsequent SEE criticality subsystems assignments as the error budget is allocated to the various potential sources (e.g., proton events in the CCD pixels, SEU in camera ADC, bits errors in the data bus, soft errors in the solid state recorder). Examples detailing this process are given in [Mars P 96]. Just as with the availability requirements already discussed, the top-level data integrity requirements could be tailored to the mission needs in terms of different performance levels for different aspects of the environment (e.g., SAA and solar event). Whenever the most demanding performance requirements can be separated from the most severe environmental conditions, mission complexity and cost can be reduced, and it is the proper expression of the top-level system requirements which allows this.

#### 5.4.3.3.2 Criticality assignments

As a part of mission planning, functional requirement definitions for each primary function are established, and this may occur without consideration of radiation effects. As part of the single event effects assessment, these same functions must be ranked

according to the degree of severity their temporary disruption or permanent loss would impose as described in Figure 23.

Functions can be broadly sorted into payload versus bus groupings. Bus functions would typically include Telemetry and Control, Power and Power Distribution, Data Bus and Mass Memory Storage, and Downlinks, whereas payload functions would tend to be more mission specific and include things such as UV/Visible imaging, Infrared imaging, Environment monitors. Obviously, all are important functions, but some (especially those associated with the bus) are clearly mission critical. Even though Telemetry and Control or other essential functions are always protected against any single point of failure by dual redundant architectures, it is usually assumed that loss of a redundant portion of a critical subsystem should not be allowed to occur due to an SEE. Thus all subsystems supporting mission critical functions would typically be designed assuming error-critical levels.

Other functions, for example a secondary experiment payload to evaluate a new technology, might be considered of less importance, and the only mission imposed requirement might be that a failure within the experiment, SEE induced or otherwise, must not affect the host. Even so, the experiment designers would likely have considerable investments in the experiment and would consequently impose their own higher level criticality to assure the success of the experiment.

In between these two extremes we have the error-vulnerable category in which a certain number of errors could be tolerated or mitigated with acceptable performance. Many satellite functions are inherently error-critical, but wherever error-critical ratings can be avoided, they should be. The error-vulnerable category allows considerable flexibility in providing acceptable performance with reliance on less expensive parts and less complex systems.

#### 5.4.3.3.3 Allocation of SEE requirements to subsystems

As the mission development progresses from planning to satellite conceptual design, the satellite functions are divided across various hardware subsystems, each of which will have to perform within certain measures to meet system top level functional requirements. Along with the division of satellite functions across these subsystems, the preliminary design phase will also include a set of derived SEE requirements which will flow out of the top level SEE requirements.

As with the case of top level requirements, the subsystem derived requirements should be expressed in terms of availability and, where appropriate, information integrity. It is the role of the team comprised of the radiation environment and effect specialists, the subsystem lead engineers, and the system engineers to establish the subsystem level derived requirements based on the subsystem function. The budgeting of availability and information integrity requirements may occur across multiple subsystems where those subsystems are functionally related. In no case should the availability or performance of the subsystem (or collection of functional related subsystems) be designed with SEE vulnerability in excess of that allowed based on the functional criticality.

However, the transmission of CCD imagery, which might be a primary mission objective, would not necessarily be deemed error-critical, and the cost associated with guaranteeing uninterrupted, error-free data might be prohibitive. In this case, availability and information integrity allowances could be applied to the function of CCD image collection and transmission in the top-level requirements. It is then the task of the engineering team to allocate this error allowance between the CCD camera, data bus, and solid state recorder subsystems. This is typically done along with functional requirements definition in the preliminary design phase, and it necessarily relies on past experience and educated guesswork with anticipation of the trades associated with the difficulty of hardening against or tolerating SEE in one subsystem versus another.

In this manner, functional requirements from the top level and associated SEE criticality levels for those functions are translated into SEE requirements at the system and subsystem hardware levels. This allocation of error allowances necessarily must occur early in the preliminary design, but it may be a dynamic process which continues into the detailed design and through test and evaluation phases. With system cost and complexity always guiding the trades, the reallocation of SEE error allowances may be required due to a number of factors, such as the availability (or cost) of SEE hardened parts or test results on candidate components indicating different sensitivities in ground radiation tests than anticipated based on initial information.

#### 5.4.3.3.4 Detailed subsystem SEE design and analysis

At this point we have established functional SEE requirements with assigned criticality levels, which in turn have been applied to error allocation budgets at the hardware subsystem level. It is now the task of the subsystem engineering team to allocate their error budgets among the various segments of the subsystem in a manner that minimizes the system cost and complexity.

The SEECA approach would now be applied to the subsystem level with the possible failure modes gauged according to what the effect might be and whether or not it reaches the boundary of the subsystem to impact the allocated error budget. In this sense, the use of SEU soft parts might be allowed even within a subsystem designated error-critical, provided error mitigation techniques within the subsystem prevented the errors from reaching the subsystem boundaries. Through this process, the error budget is managed through the completion of detailed design, and with control of cost and complexity as the driving forces.

#### **5.4.3.4 Destructive events**

Destructive SEE conditions (Single Event Latch-up, Single Event Gate Rupture, Single Event Burnout) may or may not be recoverable depending on the individual device's response. Hardening from the system level is difficult at best, and in most cases not particularly effective. Generally, parts with a non-negligible destructive SEE rate should not be used. On a case-by-case basis use of these parts with adequate circumvention methods could be authorized. Examples of mitigation methods are given in [LaBe 96].

### **5.4.3.5 Non destructive events**

Once the acceptable event rates are defined, they are compared to the device event rates. Generally a Radiation Design Margin of at least 2 is required. If a part is found to be unacceptable, the alternatives are to redesign the system (to increase the acceptable error rate) or substitute a harder part. As mentioned before, another alternative could also be the reallocation of the acceptable error rates. Examples of SEE mitigation methods are presented in [LaBe 96-2].

### **5.4.4 Particular case: Error rate prediction not possible**

For Single Event Burnout (SEB) and Single Event Gate Rupture (SEGR) of power MOSFETs, error rate prediction techniques are not mature. Hardness assurance is then based on derating of maximum operating values [Nich 96]. The values of the derating are obtained by characterization. In the past, it has been common practice to consider that up to 200V devices, a 50% derating of maximum operating values would not lead to any SEB sensitivity. This is no longer true on some new technologies. A test is recommended on any new device to define the acceptable derating.

## **6.0 MANAGEMENT OF HARDNESS ASSURANCE**

### **6.1 Introduction**

Figure 25 shows the different groups who interact in order to form a spacecraft design team. It shows that a large number of people, factors, and considerations go into a system design. Conflicts between the requirements for different environments are resolved through trade-off in design studies. The arrangements for resolving conflicts and getting the work done are contained in a series of project documents. This system of requirements and reviews forces the hardware designers and builders to implement the design features required to meet success criteria.

There are many ways of managing the process of hardness assurance described in the previous chapters. The options are a centralized radiation effects management or a devolved management, in which subsystem engineers are responsible for all environmental constraints. The latter option is generally used for space systems. Requirements are reflected through a Radiation Environment specification and a Radiation Hardness specification, which define the external environment, the techniques to be used and the radiation design margin required. At NASA-GSFC a lead radiation engineer is assigned to each space flight project. The RHA engineering process is viewed in a manner similar to that used by a mechanical or a thermal engineer who is assigned for the life of a project. With a single point of contact for all project radiation issues (environment, device selection, testing) each program has a radiation effects expert responsible for ensuring performance in the radiation environment. By participating early in flight programs, the radiation effects engineer may contribute to cost reduction strategies.

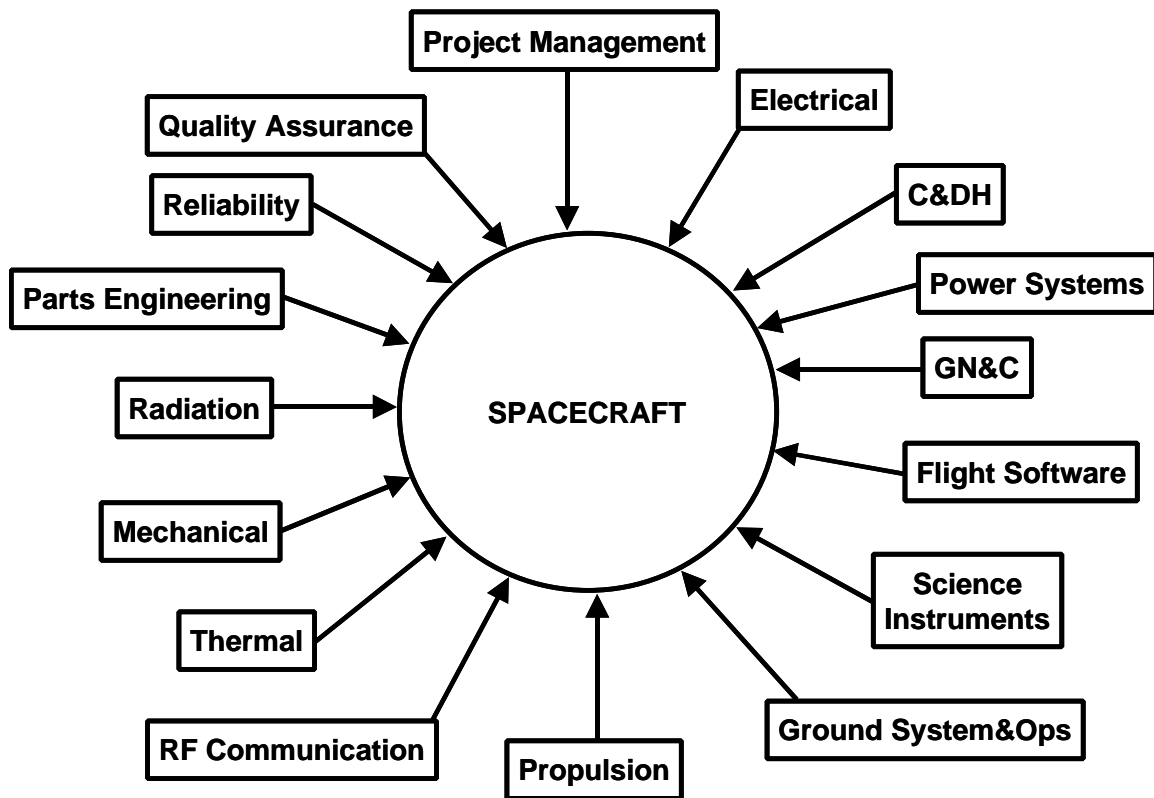


Figure 25: Typical spacecraft design team.

## 6.2 Radiation specifications

### 6.2.1 Introduction

The two primary documents related to radiation effects analysis are the radiation environment specification and the Radiation hardness specification. These two documents could be merged into a single document. The parts top-level requirements are also reflected on the Parts Control Plan document.

### 6.2.2 Radiation Environment specification

The radiation environment specification for the mission should include:

- a) The unshielded mission-average proton and electron energy spectra from trapped radiation.
- b) The unshielded fluence spectrum of solar protons for the complete mission. Appropriate geomagnetic shielding shall be applied.
- c) The unshielded worst-case instantaneous energy spectra of trapped electrons, trapped protons and solar energetic protons (geomagnetically shielded) for the mission, for internal charging and sensor interference analysis.
- d) The mission-average and peak trapped proton spectra for nominal shielding.
- e) The GCR ion LET spectrum for the appropriate solar cycle phase. A LET spectrum for the peak, worst day and worst week solar particle event. The LET spectrum shall

- include contributions from all ions from  $Z=1$  to  $Z=92$ . Appropriate geomagnetic shielding shall be applied. Appropriate material shielding shall be applied.
- f) A mission dose versus shielding depth curve or table for dose at the center of a solid Aluminum sphere, including contributions from trapped electrons and protons, solar energetic protons and electron-induced bremsstrahlung.
  - g) The damage-equivalent fluences of 1 MeV electrons and 10 MeV protons for solar cell damage estimates.
  - h) NIEL 10 MeV equivalent fluences for CCD, optoelectronic and optical components as a function of spherical shielding depth.

### **6.2.3 Radiation Hardness assurance specification**

A Hardness Assurance specification for the mission should include at minimum:

- a) the mission top level requirements.
- b) the required Radiation Design Margins.
- c) the test requirements.

### **6.3 Radiations reviews**

The two main reviews of a project are the Preliminary Design Review (PDR) and the Critical Design Review (CDR). Radiation problems are covered in these reviews. In the reviews the following topics as appropriate should be covered:

- At PDR:
  - The proposed mechanical layout to achieve maximum inherent shielding; trade-off with thermal control, cabling, fabrication and test efficiencies.
  - The electronic design approach, including circuit design rules, electronic parts sensitivity and test requirements, and parts selection parameters.
  - The preliminary shielding analysis.
- At CDR
  - The results of radiation tests.
  - The materials and special parts sensitivity, including special application/screening .
  - The radiation problems previously identified.
  - The circuit design analysis results.
  - The final shielding analysis.
  - The expected radiation design margins.

Other reviews could be organized to solve specific problems. The purpose of a review is to get the experts from different disciplines together so they can help the system designers to make the proper decisions.

One of the main problems in space programs is that sometimes the radiation characterization results arrive after the CDR. This could have a significant impact on the project cost and schedule, when the results lead to design modifications after the CDR.

## **6.4 Waivers**

Waivers trade risk against project resources or modify requirements for a specific situation. In a situation where the solutions to a problem are being developed, waivers are used to track all those subsystems affected by the requirement. When requirements are not met, waivers are required, in particular when the RDM is not met [Holm 93]. For example, a radiation test that might arrive late in the program development and show a SET sensitivity that will be a concern for a particular application. The risk is evaluated and, rather than undertaking a costly retrofit, the subsystem manufacturer may issue a waiver that documents the problem and asks the project to relax the functional requirement of this subsystem. The project will evaluate the risk and make a decision to accept or reject this waiver request.

## **7.0 EMERGING RADIATION HARDNESS ASSURANCE ISSUES**

During the last ten years, we have seen the emergence of commercial off-the-shelf (COTS) parts and emerging new technologies in space programs. The first COTS parts to fly in space, were memories for use in Solid State Recorders (SSR). Today, the use of COTS is common practice. Radiation Hardness methodologies have been adapted with the usage of COTS [LaBe 98]. Most of the significant points have been addressed in this course.

The main concern with COTS is the variability and the unpredictability of the radiation response due to the limited control and frequent processing changes. For COTS it is always necessary to test the flight lot. This is a significant programmatic constraint because the radiation results may be only available in the last phases of the project development, and the impact of bad radiation results may be significant. If there is often a way to deal with bad TID results via spot shielding, it is not the same for SEE effects. Therefore it is important that the design engineers know at the beginning of the program all of the potential radiation hazards in order to implement tolerant designs. Another way to deal with this problem is to make single buys for Engineering Models (EM) and flight models (FM) and test different possible candidates early in the program. This approach, if used systematically, may be costly. Again, a good knowledge of the possible radiation hazards and the possible impacts on the subsystems will help to make the good decisions.

Another issue with emerging technologies is their increased complexity and performance. This results in new radiation sensitivities [LaBe 98, John 97]. For example, Single Event Functional Interrupt (SEFI) is now a common failure mode. First observed on processors, now SEFI is observed on Synchronous Dynamic Random Access Memories (SDRAM) [Koga 01] and Analog to Digital Converters (ADC). Removal of power supply and subsequent re-initialization are required to resume proper operation. The increased clock speed and complexity are also major challenges for radiation testing. This makes the tests more expensive and longer to perform. Sometimes, it is very difficult to test the full performance of a part. For example, to test the full accuracy of a 16 bits ADC, a measurement accuracy of tens of micro volts is necessary. This accuracy is very difficult to achieve in the noisy environment of a heavy ion accelerator. In the future, design engineers will have to be more involved in the radiation tests to solve these problems.

The new packaging technologies are also an important issue. First, the high number of input and outputs is another test complexity. Second, some package technologies are problematic for SEE testing. For example, most of modern DRAMs have a 150  $\mu\text{m}$  thick lead frame that covers the whole die area [Koga 00]. Another example is the PENTIUM III processor where the sensitive region on the part is only accessible through the backside of the die because of the die mounting technology. The die has a thickness of 900  $\mu\text{m}$  [Howa 01]. The heavy ion accelerators currently used for SEE testing provide ions with a penetration range in the order of tens of  $\mu\text{m}$ . This is not sufficient for some devices and there is a need for higher energy beams with longer penetration ranges [Poiv 01].

## **8.0 CONCLUSION**

The two main activities of a radiation hardness assurance program are the definition of the radiation environment at the part level and the definition of the part failure level. As more and more TID sensitive parts are used, a top-level requirement is usually not sufficient except for programs with low TID requirements. An accurate spacecraft modeling and a 3-D sectoring/ray trace or Monte Carlo radiation analysis allows a significant reduction of the TID requirement. Another advantage of having a spacecraft model is the ability to analyze the effectiveness of mitigation techniques, e.g., moving boxes to locations that offer more protection or adding spot shielding to parts.

The radiation characterization is the first step of the definition of the part failure level. Then, the part radiation sensitivity is compared to the part uses in the different applications and the impact at the circuit level, box level, subsystem level, and system level. Design mitigation techniques allow the use of radiation sensitive parts.

All these activities affect the spacecraft and electronic box layout, the system design, and even system operations. The radiation hardness assurance process is no longer confined to the part level. Radiation hardness has to be taken into account at all the stages of the system development. Taking into account the hardness assurance in the early phases of a program development will allow reducing significantly the costs of hardness assurance.

The reader should also keep in mind that there are a lot of uncertainties in this process: in the environment definition, in the simulation of this environment at ground level, and in the part characterization [Stas 91]. All these uncertainties are put in the radiation design margin. To quote Andrew Holmes Siedle and Len Adams [Holm 93], “The recipe for restful nights is an RDM value well above 2.”

## **9.0 ACKNOWLEDGEMENTS**

This section of the short course would not have been possible without the consistent support and friendship of colleagues at NASA-GSFC. Special thanks go to Martha O’Bryan for the help on the graphics and slides, to Janet Barth and Ken LaBel for their support and encouragement, and Stass for long hours of tutorial. Ron Pease has been of great help for providing materials and his excellent advice. Thanks go to ASTRIUM radiation group and especially Renaud Mangeret for providing materials, to Paul

Dressendorfer for his advice and, Brian Bolger for kindly editing this text. Most of all, I am thankful to my wife for her support and patience the last 7 months.

## 10.0 REFERENCES

- [Adam 86] J.H. Adams, "Cosmic Ray Effects on Microelectronics, Part IV," NRL Memorandum Report 5901, Naval Research Laboratory, Washington DC 20375-5000, USA, 1986.
- [Ansp 96] B.E. Anspaugh, "GaAs Solar Cell Radiation Handbook," JPL Publication 96-9, 1996.
- [Astr 01] "Impact des Proprietes Effectives des Materiaux et Structures de Blindage sur le Calcul de Niveaux de Dose," ASTRIUM report AIN.RA.RM.705.102.01, Jan. 2001.
- [Bara 00] J. Barak, "Empirical Modeling of Proton Induced SEE Rates," *IEEE Trans. Nucl. Sci.*, vol. 47, n°3, pp. 545-550, Jun. 2000.
- [Bart 96] J. Barth, "Ionizing Radiation Environment Concerns," SEECA Single Event Effect Criticality Analysis, <http://radhome.gsfc.nasa.gov/radhome/papers/seecai.htm>, 1996.
- [Bart 97] J. Barth, "Modeling Space Radiation Environments," 1997 IEEE NSREC short course, Snowmass, Jul. 1997.
- [Beau 94] J. Beaucour, T. Carriere, A. Gach, D. Laxague, and P. Poirot, "Total Dose Effects on Negative Voltage Regulator," *IEEE Trans. Nuc. Sci.*, vol. 41, n°6, pp. 2420-2426, Dec. 1994.
- [Bono 97] L. Bonora, J. P. David, "An attempt to define conservative conditions for total dose evaluation of bipolar ICs," *IEEE Trans. Nucl. Sci.*, vol. 44, n°6, pp. 1974-1980, Dec. 1997.
- [Buch 96] S. Buchner, D. Mc Morrow, J. Melinger, and A. B. Campbell, "Laboratory Tests for Single Event Effects," *IEEE Trans. Nucl. Sci.*, vol. 43, n°2, pp. 678-686, Apr. 1996.
- [Carr 95] T. Carriere, J. Beaucour, A. Gach, B. Johlander, and L. Adams, "Dose Rate and Annealing Effects on Total Dose Response of MOS and Bipolar Circuits," *IEEE Trans. Nucl. Sci.*, vol. 42, n°6, pp. 2567-2574, Dec. 1995.
- [Carr 00] T. Carriere, R. Ecoffet, and P. Poirot, "Evaluation of Accelerated Total Dose Testing of Linear Bipolar Circuits," *IEEE Trans. Nucl. Sci.*, vol. 47, n°6, pp. 2350-2357, Dec. 2000.
- [Calv 96] P. Calvel, C. Barillot, P. Lamothe, R. Ecoffet, S. Duzellier, and D. Falguere, "An Empirical Model for Predicting Proton Induced Upset," *IEEE Trans. Nucl. Sci.*, vol. 43, n°6, pp. 2827-2832, Dec. 1996.
- [Clar 95] S. Clark, J. P. Bings, M. C. Maher, M. K. Williams, D. R. Alexander, and R. L. Pease, "Plastic Packaging and Burn-in Effects on Ionizing Dose Response in CMOS Microcircuits," *IEEE Trans. Nuc. Sci.*, vol. 42, n°6, pp. 1607-1614, Dec. 1995.
- [Daly 89] E. J. Daly, "The Radiation Environment; The Interaction of Radiation with Materials," computer methods ESA, 1989.
- [Daly 96] E. J. Daly, J. Lemaire, D. Heynderickx, and D. J. Rodgers, "Problems with Models of the Radiation Belts," *IEEE Trans. Nucl. Sci.*, vol. 43, n°2, pp. 403-415, Apr. 1996.

- [Douc 95] B. Doucin, T. Carriere, C. Poivey, P. Garnier, J. Beaucour, "Model of Single Event Upsets Induced by Space Protons in Electronic Devices," RADECS 1995 proceedings, pp. 402-408, 1996.
- [Dowl 93] S. Dowling, "Comparative Effect of Gamma Total Dose on Surface Mount and Non Surface Mount Bipolar Transistors," RADECS 1993 Proceedings, pp. 338-343, 1994.
- [Duze 96] S. Duzellier, R. Ecoffet, "Recent Trends in Single Event Effect Ground Testing," *IEEE Trans. Nucl. Sci.*, vol. 43, n<sup>o</sup>2, pp. 671-677, Apr. 1996.
- [ECSS 00] European Cooperation for Space Standardization (ECSS), "Space Engineering, Space Environment," ECSS-E-10-04A, Jan. 2000.
- [Feyn 93] J. Feynman, G. Spitale, J. Wang and S. Gabriel, "Interplanetary Proton Fluence Model: JPL 1991," *J. Geophys. Res.* 98, A8, pp. 13281-13294, 1993.
- [Gate 96] M. Gates, "Single Event Effect Criticality Analysis (SEECA) Functional Analysis and Criticality," <http://radhome.gsfc.nasa.gov/radhome/papers/seecai.htm>, 1996.
- [Holm 93] A. Holmes-Siedle, and L. Adams, "Handbook of Radiation Effects," Oxford University Press, 1993.
- [Hopk 96] G.R. Hopkinson, C.J. Dale, and P. W. Marshall, "Proton effects in Charge Coupled Devices," *IEEE Trans. Nucl. Sci.*, vol. 43, n<sup>o</sup>2, pp. 614-627, Apr. 1996.
- [How 2001] J.W. Howard, M. A. Carts, R. Stattel, C. E. Rogers, T. L. Irwin, C. Dunsmore, J. A. Sciarini, and K. A. LaBel, "Total Dose and Single Event Effects Testing of the Intel Pentium III (P3) and AMD K7 Microprocessors," IEEE NSREC 2001, dataworkshop proceedings, pp. 38-47, 2001.
- [Hust 98] S. L. Huston, and K. A. Pfitzer, "A New Model for the Low Altitude Trapped Proton Environment," *IEEE Trans. Nuc. Sci.*, vol. 45, n<sup>o</sup>6, pp. 2972-2978, Dec. 1998.
- [John 94] A. H. Johnston, G. M. Swift, and B. G. Rax, "Total Dose Effects in Conventional Bipolar Transistors and Linear Integrated Circuits," *IEEE Trans. Nuc. Sci.*, vol. 41, n<sup>o</sup>6, pp. 2427-2436, Dec. 1994.
- [John 95] A. H. Johnston, B. G. Rax, and C. I. Lee, "Enhanced Damage in Linear Bipolar Integrated Circuits at Low Dose Rates," *IEEE Trans. Nuc. Sci.*, vol. 42, n<sup>o</sup>6, pp. 1650-1659, Dec. 1995.
- [John 96] A.H. Johnston, "Single Event Effect Criticality Analysis (SEECA) Effects in Electronic Devices and SEE Rates," <http://radhome.gsfc.nasa.gov/radhome/papers/seecai.htm>, 1996.
- [John 97] A. H. Johnston, "Radiation Effects in Advanced Microelectronics Technologies," RADECS 1997 Proceedings, pp. 1-16, 1998.
- [Jord 82] T. Jordan, "NOVICE a Radiation Transport/Shielding Code," Experimental and Mathematical Physics Consultants, Report #EMP.L82.001, Jan. 1982.
- [King 74] J.H. King, "Solar proton fluences for 1977-1983 Space Missions," *J. Spacecrafts and Rockets*, 11, 401, 1974.
- [Koga 96] R. Koga, "Single Event Effect Ground Test Issues," *IEEE Trans. Nucl. Sci.*, vol. 43, n<sup>o</sup>2, pp. 661-670, Apr. 1996.

- [Koga 00] R. Koga, S. H. Crain, P. Yu, and K. B. Crawford, "SEE Sensitivity Determination of High Density DRAMs with Limited Range Heavy Ions," IEEE NSREC 2000, dataworkshop proceedings, pp. 45-52, 2000.
- [Koga 01] R. Koga, P. Yu, K. B. Crawford, S. H. Crain, and V.T. Tran, "Permanent Single Event Functional Interrupts (SEFI) in 128 and 256 Mbit Synchronous Dynamic Random Access Memories (SDRAMs)," IEEE NSREC 2001, dataworkshop proceedings, pp. 6-13, 2001.
- [LaBe 96] K. LaBel, "SEECA Single Event Effect Criticality Analysis, SEU propagation analysis: system level effects," <http://radhome.gsfc.nasa.gov/radhome/papers/seecai.htm>, 1996.
- [LaBe 96-2] K. LaBel, and M. Gates, "Single-Event-Effect Mitigation From a System Perspective," *IEEE Trans. Nucl. Sci.*, vol. 43, n<sup>o</sup>2, pp. 654-660, Apr. 1996.
- [LaBe 98] K. A. LaBel, A. H. Johnston, J. L. Barth, R. A. Reed, and C. E. Barnes, "Emerging Radiation Hardness Assurance (RHA) issues: A NASA Approach for Space Flight Programs," *IEEE Trans. Nucl. Sci.*, vol. 45, n<sup>o</sup>6, pp. 2727-2736, Dec. 1998.
- [McCl 94] S. Mc Clure, R. L. Pease, W. Will, and G. Perry, "Dependence of Total Dose Response of Bipolar Linear Microcircuits on Applied Dose Rate," *IEEE Trans. Nuc. Sci.*, vol. 41, n<sup>o</sup>6, pp. 2544-2549, Dec. 1994.
- [McLe 87] F. Mc lean, and T. Oldham, "Basic Mechanisms of Radiation Effects on Electronic Materials, Devices and Integrated Circuits," 1987 IEEE NSREC short course, Snowmass, Jul. 1987.
- [Mang 96] R. Mangeret, T. Carriere, and J. Beaucour, "Effects of Material and/or Structure on Shielding of Electronic Devices," *IEEE Trans. Nucl. Sci.*, vol. 43, n<sup>o</sup>6, pp. 2665-2670, Dec. 1996.
- [Mars C. 99] C. Marshall, and P. Marshall, "Proton Effects and Test Issues for Satellite Designers, part B: Displacement Effect," 1999 IEEE NSREC short course, Norfolk, Jul. 1999.
- [Mars P. 96] P. Marshall, "SEECA, SEE Criticality Assessment Case Studies," <http://radhome.gsfc.nasa.gov/radhome/papers/seecai.htm>, 1996.
- [Mars P. 02] P. Marshall, "Electronics Radiation Characterization Project Task on Photonic Technology. Rate Prediction Tool Assessment for Single Event Transient Errors," NASA-GSFC report, Jan. 2002.
- [Marv 00] D. C. Marvin, and J. C. Nocerino, "Evaluation of Multijunction Solar Cell Performance in Radiation Environments," Photovoltaic Specialist Conference 2000, Conference Record for the 28<sup>th</sup> IEEE, pp. 1102-1105, 2000.
- [Mess 92] G. Messenger, M. Ash, "The Effects of Radiation on Electronics Systems," 2<sup>nd</sup> edition, Van Nostrand Reinhold, 1992.
- [Miro 98] V.V. Miroshkin, M. G. Tverskoy, "A Simple Approach to SEU Cross Section Evaluation," *IEEE Trans. Nucl. Sci.*, vol. 45, n<sup>o</sup>6, pp. 2884-2890, Dec. 1998.
- [Mour 94] I. Mouret, M. Allenspach, R. D. Schrimpf, J. R. Brews, K. F. Galloway, and P. Calvel, "Temperature and Angular Dependence of Substrate Response in SEGR," *IEEE Trans. Nucl. Sci.*, vol. 41, n<sup>o</sup>6, p. 2216-2221, Dec. 1994.
- [Nich 96] D.K. Nichols, J. R. Coss, T. Miyahira, J. Titus, D. Oberg, J. Wert, P. Majewski, J. Lintz, "Update of Single Event Failures in Power MOSFETs," 1996 IEEE radiation effects data workshop, pp. 67-72, 1996.

- [Peas 94] R. L. Pease, and D. R. Alexander, "Hardness Assurance for Space Systems Microelectronics," *Rad. Phys. Chem.*, vol. 43, n° ½, pp. 191-204, 1994.
- [Peas 96] R. L. Pease, "Total Dose Issues for Microelectronics in Space Systems," *IEEE Trans. Nucl. Sci.*, vol. 43, n°2, pp. 442-452, Apr. 1996.
- [Peas 96-2] R. L. Pease, M. Gehlhausen, "Elevated Temperature Irradiation of Bipolar Linear Microcircuits," *IEEE Trans. Nucl. Sci.*, vol. S43, n°6, p. 3161-3166, Dec. 1996.
- [Peas 96-3] R.L. Pease, W. E. Combs, A. Johnston, T. Carriere, C. Poivey, A. Gach, and S. Mc Clure, "A Compendium of Recent Total Dose Data on Bipolar Linear Circuits," 1996 IEEE Radiation Effects Data Workshop, pp. 28-37, 1996.
- [Peas 98] R. Pease, M. Gehlhausen, J. Krieg, J. Titus, T. Turflinger, D. Emily, and L. Cohn, "Evaluation of Proposed Hardness Assurance Method for Bipolar Linear Circuits with Enhanced Low Dose Rate Sensitivity (ELDRS)," *IEEE Trans. Nucl. Sci.*, vol. 45, n°6, pp. 2665-2672, Dec. 1998.
- [Peas 01] R.L. Pease, A. Sternberg, L. Massengill, R. Schrimpf, S. Buchner, M. Savage, J. Titus, and T. Turflinger, "Critical Charge for Single Event Transients (SET) in Bipolar Linear Circuits," *IEEE Trans. Nucl. Sci.*, vol. 48, n°6, pp. 1966-1972, Dec. 2001.
- [Peas 01-2] R.L. Pease, "Radiation Effects Short Course Hardness Assurance," Vanderbilt University, August 2001.
- [Peas 01-3] R.L. Pease, S. Mc Clure, A. H. Johnston, J. Gorelick, T.L. Turflinger, M. Gehlhausen, J. Krieg, T. Carriere, and M. Shaneyfelt, "An Updated Data Compendium on Enhanced Low Dose Rate Sensitive (ELDRS) Bipolar Linear Circuits," 2001 IEEE Radiation Effects Data Workshop, pp. 127-133, 2001.
- [Pete 92] E.L. Petersen, "The Relationship of Proton and Heavy Ion Upset Thresholds," *IEEE Trans. Nucl. Sci.*, vol. 39, n°6, pp. 1600-1604, Dec. 1992.
- [Pick 96] J. Pickel, "Single Event Effects Rate prediction," *IEEE Trans. Nuc. Sci.*, vol. 43, n°2, pp. 483-495, Apr. 1996.
- [Poiv 95] C. Poivey, O. Notebaert, P. Garnier, T. Carriere, J. Beaucour, B. Steiger, J. M. Salle, F. Bezerra, R. Ecoffet, B. Cadot, M. C. Calvet, P. Simon, "Proton SEU Test of MC68020, MC68882, TMS 320C25 on the ARIANE5 Launcher On Board Computer (OBC) and Inertial Reference System (SRI)," RADECS 1995 proceedings, pp. 289-295, 1996.
- [Poiv 00] C. Poivey, B. Doucin, T. Carriere, P. Calvel, and R. Marec, "Heavy Ion Induced Gigantic Multiple Errors in State of the Art Memories," 4<sup>th</sup> ESA Electronic Component Conference (EECC), Noordwijk, The Netherlands, Apr. 2000.
- [Poiv 01] C. Poivey, J. A. Barth, R. A. Reed, K. A. LaBel, E. Stassinopoulos, and M. Xapsos, "Implications of Advanced Microelectronics Technologies for Heavy Ion Single Event Effect (SEE) Testing," to be published in RADECS 2001 proceedings.
- [Poiv 02] C. Poivey, S. Buchner, K. LaBel, J. Howard, and J. Forney, "Single Event Transient (SET) in Linear Devices, Testing Guidelines," SEE symposium, 2002.
- [Poug 00] V. Pouget, "Simulation Experimentale par Impulsions Laser Ultra Courtes des Effets des Radiations Ionisantes sur les Circuits Integres," Thesis ref 2250, Jul. 2000.
- [Reed 98] R. A. Reed, P. W. Marshall, A. H. Johnston, J. L. Barth, C. J. Marshall, K. A. LaBel, M. D'O'dine, H. S. Kim, and M. A. Carts, "Emerging Optocoupler Issues with Energetic

- Particle-Induced Transients and Permanent Radiation Degradation,” *IEEE Trans. Nuc. Sci.*, vol. 45, n°6, pp. 2833-2841, Dec. 1998.
- [Reed 01] R. A. Reed, C. Poivey, P. W. Marshall, K. A. LaBel, C. J. Marshall, S. Kniffin, J. L. Barth, and C. Seidleck, “Assessing the Impact of the Space Radiation Environment on Parametric Degradation and Single-Event Transients in Optocouplers,” *IEEE Trans. Nuc. Sci.*, vol. 48, n°6, pp. 2202-2209, Dec. 2001.
- [Reed 02] R. A. Reed, “Guideline for Ground Radiation Testing and Using Optocouplers in the Space Radiation Environment,” NASA-GSFC report, Mar. 2002.
- [Roll 90] J. G. Rollins, “Estimation of Proton Upset Rate from Heavy Ion Test Data,” *IEEE Trans. Nucl. Sci.*, vol. 37, n°6, pp. 1961-1965, Dec. 1990.
- [Sawi 76] D.M. Sawyer, and J.I. Vette, “AP8 Trapped Proton Environment for Solar Maximum and Solar Minimum,” NSSDC/WDC-A-R&S 76-06, NASA-GSFC, 1976.
- [SEEC 96] NASA-GSFC Single Event Effect Criticality Analysis, 1996, <http://radhome.gsfc.nasa.gov/radhome/papers/seecai.htm>
- [Selt 80] S. Seltzer, “SHIELDOSE: A computer Code for Space Shielding Radiation Dose Calculations,” NBS Technical Note 1116, National Bureau of Standards, May 1980.
- [Shan 94] M. Shaneyfelt, D. M. Fleetwood, J. R. Schwank, T. L. Meisenheimer, and P. S. Winokur, “Effects of burn-in on radiation hardness,” *IEEE Trans. Nuc. Sci.*, vol. 41, n°6, pp. 2550-2559, 1994.
- [Stas 91] E. G. Stassinopoulos, G. J. Brucker, “Shortcomings in Ground Testing, Environment simulations, and Performance Predictions for Space Applications,” RADECS 1991 Proceedings, pp. 3-16, 1992.
- [Stas 92] E.G. Stassinopoulos, G. J. Brucker, P. Calvel, A. Baiget, C. Peyrotte, R. Gaillard, “Charge Generation by Heavy Ions in Power MOSFETs Burnout Space Predictions, and Dynamic SEB Sensitivity,” *IEEE Trans. Nuc. Sci.*, vol. 39, n°6, pp. 1704-1711, Dec. 1992.
- [Stas 96] E.G. Stassinopoulos, G. J. Brucker, D. W. Nakamura, C. A. Stauffer, and J. L. Barth, “Solar Flare Proton Evaluation at Geostationary Orbits for Engineering Applications,” *IEEE Trans. Nuc. Sci.*, vol. 43, n°2, pp. 369-382, Apr. 1996.
- [Tada 82] H.Y. Tada, J. R. Carter, B. E. Anspaugh, and R. G. Downing, “Solar cell radiation handbook,” 3<sup>rd</sup> Edition, JPL publication 82-69, 1982.
- [Tastet 91] P. Tastet, J. Garnier., “Heavy ion Sensitivity of Power Mosfets,” RADECS 1991 proceedings, pp. 138-142, 1992.
- [Titu 95] J.L. Titus, C. F. Wheatley, I. Mouret, M. Allenspach, J. Brews, R. Schrimpf, K. Galloway, and R. L. Pease, “Impact of Oxide Thickness on SEGR Failure in Vertical Power MOSFETs; Development of a Semi-empirical Expression,” *IEEE Trans. Nuc. Sci.*, vol. 42, n°6, pp. 1928-1934, Dec. 1995.
- [Tran 92] C. Tranquille, E. J. Daly, "An evaluation of solar-proton Event Models for ESA missions," *ESA Journal* 1992, vol. 16, pp 275-297.
- [Trus 2000] P. Truscott, F. Lei, C. Dyer, C. Ferguson, R. Gurriaran, P. Nieminen, E. Daly, J. Apostokalis, S. Giani, M. Grazia Pia, L. Urban, and M. Maire, “GEANT4 – A new Monte Carlo Toolkit for Simulating Space Radiation Shielding and Effects,” IEEE NSREC 2000 data workshop proceeding, pp. 147-152, 2000.

- [Tylk 97] A.J. Tylka, J. H. Adams, P. R. Boberg, B. Brownstein, W. F. Dietrich, E. O. Flueckiger, E. L. Petersen, M. A. Shea, D. F. Smart, and E. C. Smith, "CREME96: a Revision of the Cosmic Ray Effects on Micro-Electronics Code," *IEEE Trans. Nuc. Sci.*, vol. 44, n°6, pp. 2150-2160, Dec. 1997.
- [Vett 91] J.I. Vette, "The AE-8 Trapped Electron Model Environment," NSSDC/WDC-A-R&S 91-24, NASA-GSFC, 1991.
- [Wino 93] P. S. Winokur, M. R. Shaneyfelt, T. L. Meisenheimer, and D. M. Fleetwood, "Advanced qualification techniques," RADECS 1993 proceedings, pp. 289-299, 1994.
- [Witc 97] S.C. Witczak, R. D. Schrimpf, D. M. Fleetwood, K. F. Galloway, R. C. Laco, D. C. Mayer, J. M. Puhl, R. L. Pease, and J. Suehle, "Hardness Assurance Testing of Bipolar Junction Transistors at Elevated Irradiation Temperatures," *IEEE Trans. Nuc. Sci.*, vol. 44, n°6, pp. 1989-2000, Dec. 1997.
- [Xaps 99- 1] M. A. Xapsos, G.P. Summers, J. L. Barth, E. G. Stassinopoulos, and E.A. Burke, "Probability Model for Worst Case Solar Proton Event Fluences," *IEEE Trans. on Nuc. Sci.*, vol. 46, n° 6, pp. 1481-1485, Dec. 1999.
- [Xaps 99-2] M.A. Xapsos, J. L. Barth, E. G. Stassinopoulos, "Space Environment Effects: Model for Emission of Solar Protons (ESP) – cumulative and worst case event fluences," NASA report NASA/TP-1999-209763, Dec. 1999.
- [Xaps 00] M.A. Xapsos, G. P. Summers, J.L. Barth, E.G. Stassinopoulos, E.A. Burke, "Probability Model for Cumulative Solar Proton Event Fluences," *IEEE Trans. on Nuc. Sci.*, vol. 47, n° 3, pp. 486-490, Jun. 2000.